

**An Alternative Three-Term Decomposition for Single
Crystal Deformation Motivated by Non-Linear Elastic
Dislocation Solutions**

by J. D. Clayton

ARL-RP-478

April 2014

A reprint from the *Quarterly Journal of Mechanics and Applied Mathematics*, Vol. 67, No. 1,
pp. 127–158, 2014.

NOTICES

Disclaimers

The findings in this report are not to be construed as an official Department of the Army position unless so designated by other authorized documents.

Citation of manufacturer's or trade names does not constitute an official endorsement or approval of the use thereof.

Destroy this report when it is no longer needed. Do not return it to the originator.

Army Research Laboratory

Aberdeen Proving Ground, MD 21005-5069

ARL-RP-478

April 2014

An Alternative Three-Term Decomposition for Single Crystal Deformation Motivated by Non-Linear Elastic Dislocation Solutions

J. D. Clayton

Weapons and Materials Research Directorate, ARL

A reprint from the *Quarterly Journal of Mechanics and Applied Mathematics*, Vol. 67, No. 1,
pp. 127–158, 2014.

REPORT DOCUMENTATION PAGE			Form Approved OMB No. 0704-0188		
Public reporting burden for this collection of information is estimated to average 1 hour per response, including the time for reviewing instructions, searching existing data sources, gathering and maintaining the data needed, and completing and reviewing the collection information. Send comments regarding this burden estimate or any other aspect of this collection of information, including suggestions for reducing the burden, to Department of Defense, Washington Headquarters Services, Directorate for Information Operations and Reports (0704-0188), 1215 Jefferson Davis Highway, Suite 1204, Arlington, VA 22202-4302. Respondents should be aware that notwithstanding any other provision of law, no person shall be subject to any penalty for failing to comply with a collection of information if it does not display a currently valid OMB control number. PLEASE DO NOT RETURN YOUR FORM TO THE ABOVE ADDRESS.					
1. REPORT DATE (DD-MM-YYYY) April 2014		2. REPORT TYPE Reprint		3. DATES COVERED (From - To) January 2013–January 2014	
4. TITLE AND SUBTITLE An Alternative Three-Term Decomposition for Single Crystal Deformation Motivated by Non-Linear Elastic Dislocation Solutions			5a. CONTRACT NUMBER		
			5b. GRANT NUMBER		
			5c. PROGRAM ELEMENT NUMBER		
6. AUTHOR(S) J. D. Clayton			5d. PROJECT NUMBER AH80		
			5e. TASK NUMBER		
			5f. WORK UNIT NUMBER		
7. PERFORMING ORGANIZATION NAME(S) AND ADDRESS(ES) U.S. Army Research Laboratory ATTN: RDRL-WMP-C Aberdeen Proving Ground, MD 21005-5069			8. PERFORMING ORGANIZATION REPORT NUMBER ARL-RP-478		
9. SPONSORING/MONITORING AGENCY NAME(S) AND ADDRESS(ES)			10. SPONSOR/MONITOR'S ACRONYM(S)		
			11. SPONSOR/MONITOR'S REPORT NUMBER(S)		
12. DISTRIBUTION/AVAILABILITY STATEMENT Approved for public release; distribution is unlimited.					
13. SUPPLEMENTARY NOTES A reprint from the <i>Quarterly Journal of Mechanics and Applied Mathematics</i> , Vol. 67, No. 1, pp. 127–158, 2014.					
14. ABSTRACT A new third term is incorporated within the multiplicative decomposition of the deformation gradient in the context of geometrically non-linear mechanics of defective elastic-plastic crystals. This enhanced description, when applied to an element of material of finite volume, accounts explicitly for average local residual lattice distortion due to defects within that volume. The magnitude of the distortion from this third term, determined analytically for an elastic cylindrical volume of outer radius R containing a single dislocation line threading its centre, is estimated as $\{[b/(\pi R)]^2 + f^2 + g^2\}^{1/2}$, where b is Burgers vector magnitude, f accounts for elastic non-linearity, and g accounts for core effects. For a straight screw dislocation in a third-order isotropic elastic medium, at a dislocation density of 10 per cent of theoretical maximum, $b/(\pi R)$ is on the order of 0.1, f on the order of 0.01 and g is proportional to pressure exerted by the core and can be significant. Predictions of stresses and dislocation density under simple shear and uniaxial compression demonstrate differences from those of usual crystal plasticity at large strain and for high hardening. Besides offering a natural and precise delineation of contributions from dislocation velocity and dislocation generation to irreversible deformation, the three-term model allows for residual elastic strains—including dilatation observed in experiments and atomic simulations—not addressed by conventional two-term crystal plasticity.					
15. SUBJECT TERMS elasticity, plasticity, dislocations, metals, modeling					
16. SECURITY CLASSIFICATION OF:			17. LIMITATION OF ABSTRACT	18. NUMBER OF PAGES	19a. NAME OF RESPONSIBLE PERSON
a. REPORT	b. ABSTRACT	c. THIS PAGE	UU	38	J. D. Clayton
Unclassified	Unclassified	Unclassified			19b. TELEPHONE NUMBER (Include area code)

AN ALTERNATIVE THREE-TERM DECOMPOSITION FOR SINGLE CRYSTAL DEFORMATION MOTIVATED BY NON-LINEAR ELASTIC DISLOCATION SOLUTIONS

by J. D. CLAYTON[†]

(Impact Physics, US Army Research Laboratory, Aberdeen, MD, USA)

[Received 16 May 2013. Revise 1 November 2013. Accepted 27 November 2013]

Summary

A new third term is incorporated within the multiplicative decomposition of the deformation gradient in the context of geometrically non-linear mechanics of defective elastic-plastic crystals. This enhanced description, when applied to an element of material of finite volume, accounts explicitly for average local residual lattice distortion due to defects within that volume. The magnitude of the distortion from this third term, determined analytically for an elastic cylindrical volume of outer radius R containing a single dislocation line threading its centre, is estimated as $\{[b/(\pi R)]^2 + f^2 + g^2\}^{1/2}$, where b is Burgers vector magnitude, f accounts for elastic non-linearity, and g accounts for core effects. For a straight screw dislocation in a third-order isotropic elastic medium, at a dislocation density of 10 per cent of theoretical maximum, $b/(\pi R)$ is on the order of 0.1, f on the order of 0.01 and g is proportional to pressure exerted by the core and can be significant. Predictions of stresses and dislocation density under simple shear and uniaxial compression demonstrate differences from those of usual crystal plasticity at large strain and for high hardening. Besides offering a natural and precise delineation of contributions from dislocation velocity and dislocation generation to irreversible deformation, the three-term model allows for residual elastic strains—including dilatation observed in experiments and atomic simulations—not addressed by conventional two-term crystal plasticity.

1. Introduction

The decomposition of the total deformation gradient into a product of terms is a standard approach in finite plasticity theory. Such a decomposition into two (or more) terms is re-examined in the present work. Advancements are suggested here in an effort to refine the physical meaning of each term in the decomposition and associated contributions to internal energy of the material.

Let \mathbf{F} denote the total local deformation gradient for an element of crystalline material. For simplicity, thermal effects are omitted, gliding dislocations are the only kind of defect considered, and attention is restricted to a single crystal. Most typically, a two-term multiplicative decomposition of the form

$$\mathbf{F} = \mathbf{F}^E \mathbf{F}^P \quad (1.1)$$

is invoked, where \mathbf{F}^E quantifies elastic lattice stretch and rotation, and \mathbf{F}^P accounts for plastic slip due to dislocation glide. This decomposition was perhaps first written explicitly by Bilby *et al.* (1) and was advanced soon after by Kröner (2) in a more comprehensive paper. Several other early continuum theories of finite plasticity with dislocation density were compared in (3).

[†]<john.d.clayton1.civ@mail.mil>

Three-term decompositions, written as

$$\mathbf{F} = \mathbf{F}^E \mathbf{F}^I \mathbf{F}^P, \quad (1.2)$$

have also been proposed, where the mapping \mathbf{F}^I accounts for physics distinct from recoverable elasticity (\mathbf{F}^E) and lattice preserving slip (\mathbf{F}^P). Such a decomposition was perhaps first written explicitly by Kröner (2) and Bilby *et al.* (4), and was first considered from a thermodynamic point of view by Kratochvíl (5). In more recent years, such a three-term decomposition has been introduced in a number of works, with various definitions or derivations offered for \mathbf{F}^I (6)–(14).

A general premise (5) of three-term decompositions in the context of dislocation mechanics is that \mathbf{F}^I accounts for microstructural rearrangements that increase the internal energy of the material element relative to that of an element that has undergone slip but contains no dislocations or other defects within. Such energy would be associated with locally heterogeneous residual elastic strain fields and atomic phenomena (for example, core effects) not resolved by \mathbf{F}^E . Recent models for metal plasticity (6, 10, 11) have linked a term akin to \mathbf{F}^I to anisotropic strain hardening associated with defects within the element.

This article develops a new non-linear continuum description using three-term decomposition (1.2), with a focus on the origin of each term as it relates to the underlying crystal lattice.

2. Conceptual arguments

With reference to decomposition (1.2), the following definitions are now stated for a local volume element of crystalline material bounded by surface Σ :

\mathbf{F}^E : deformation due to traction applied to element boundary Σ ,
associated with configuration change $\bar{B} \rightarrow B$;

\mathbf{F}^I : deformation due to dislocations currently *inside* the element,
associated with configuration change $\tilde{B} \rightarrow \bar{B}$;

\mathbf{F}^P : deformation due to dislocations that have slipped through the *entire* element,
associated with configuration change $B_0 \rightarrow \tilde{B}$.

Here ‘deformation’ is used in an average sense for the element since atomic positions within the element will not change in an affine manner if defects are present or if traction along Σ is not uniform. Local configurations of the element are as follows:

B_0 : unstressed perfect lattice at some (initial) time ;

\tilde{B} : unstressed slipped lattice containing no defects;

\bar{B} : externally unstressed & internally stressed slipped lattice containing defect(s);

B : externally & internally stressed slipped lattice containing defect(s).

Representative configurations and deformation mappings for a cubic lattice with edge dislocations are illustrated in Fig. 1.

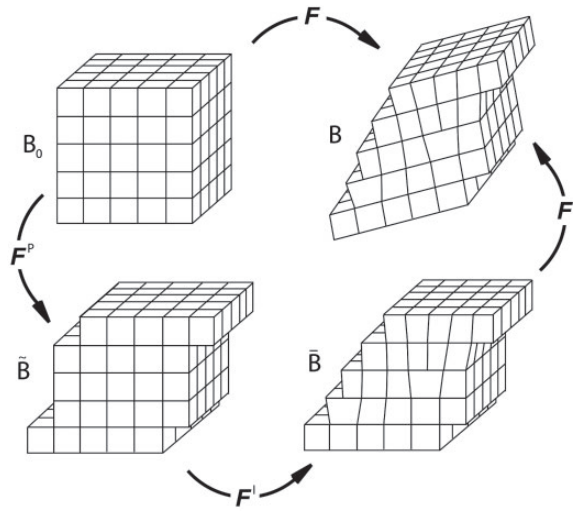


Fig. 1 Deformation mappings and configurations for a single volume element within a single crystal

Regarding reference configuration B_0 , it is assumed that the volume element is embedded within a larger slab of homogeneous material that is also unstressed in its (global) reference configuration. In this case, the element and the slab each consist of atoms arranged regularly on a perfect crystal lattice in the reference configuration. Each volume element fits exactly with its neighbours such that slab in the global reference configuration is simply connected.

A first local intermediate configuration \bar{B} of the element results from the passage of dislocations completely through the element. When separated from neighbouring elements, this element exhibits a perfect lattice, but with slip steps evident on Σ where dislocations have entered/exited. The global configuration corresponding to \bar{B} is generally disconnected.

A second local intermediate configuration \bar{B} of the element accounts for defects within that element that have not yet fully passed through. This element is free from traction along its external surface Σ , and thus is in a state of self stress. The remainder of the slab may contain defects and similar residual stresses; each element comprising the slab must, in general, be mechanically removed from its neighbours so that it too is in a state of self stress. External boundaries of the entire slab are also necessarily traction free in this global intermediate configuration.

A local current configuration B of the element is achieved when the element is stressed and deformed, along with its neighbours, so that all volume elements fit together and the body is simply connected in the global current configuration. In the local current configuration, traction must generally be applied to Σ . External surfaces of the entire slab can support traction in the global current configuration, but need not do so. If the remainder of the slab outside of the volume element contains defects, local traction may not necessarily vanish on Σ in the current configuration as a result of long-range stress fields of these defects, even if the body is globally free of applied surface and body forces.

The preceding developments are applied to a volume element containing a single edge dislocation in Section 3 and a single screw dislocation in Section 4. Generalisation to multiple defects follows in Section 5. Representative calculations using a constitutive model incorporating the present

three-term description are reported in Section 6 for several simple loading paths, followed by general discussion.

3. Edge dislocation

Consider a single edge dislocation in an isotropic elastic cylinder, as shown in Fig. 2. In an undeformed state on the left, the cylinder is of length L and radius R . Let r denote the radius of the image of the dislocation core in this undeformed state. Coordinates for the left side of Fig. 2 are $\{X, Y, Z\} = \{\rho \cos \theta, \rho \sin \theta, Z\}$; cylindrical coordinates are $\{\rho, \theta, Z\}$, where $\theta \in (-\pi, \pi]$. Boundaries of the outside of the cylinder and the core are Σ and σ , and Γ^+ and Γ^- are boundaries of the slip plane along $\{X, 0^+, Z\}$ and $\{X, 0^-, Z\}$ for $-R \leq X \leq -r$. Assume $L \gg R$ so that the problem becomes two dimensional (plane strain with $z = Z$). Let

$$b = x(X, 0^+) - x(X, 0^-) = u(X, 0^+) - u(X, 0^-), \quad -R \leq X \leq -r. \quad (3.1)$$

The magnitude of the Burgers vector is b , and $b \leq r < R$. The displacement field

$$u = x(\rho, \theta) - X, \quad v = y(\rho, \theta) - Y. \quad (3.2)$$

Assume that Σ and σ are traction free, and let ν denote Poisson's ratio. The displacement field of the exact solution to this boundary value problem in the context of linear elasticity is (15)

$$u = \frac{b}{2\pi} \left[\theta + \frac{1}{4(1-\nu)} (1 + a_1 - a_2) \sin 2\theta \right]; \quad (3.3)$$

$$v = -\frac{b}{8\pi(1-\nu)} [2(1-2\nu) \ln \rho + a_3 + (1 + a_1 - a_2) \cos 2\theta]; \quad (3.4)$$

$$a_1(\rho) = \frac{(3-4\nu)\rho^2}{R^2 + r^2}, \quad a_2(\rho) = \frac{R^2 r^2}{\rho^2(R^2 + r^2)}, \quad a_3(\rho) = \frac{2\rho^2}{R^2 + r^2}. \quad (3.5)$$

Non-zero stress components (physical cylindrical components) are $T_{\rho\rho}$, $T_{\theta\theta}$, $T_{\rho\theta}$ and $T_{zz} = \nu(T_{\rho\rho} + T_{\theta\theta})$. When $\nu \neq 0$, replacement of the plane strain boundary condition with free end

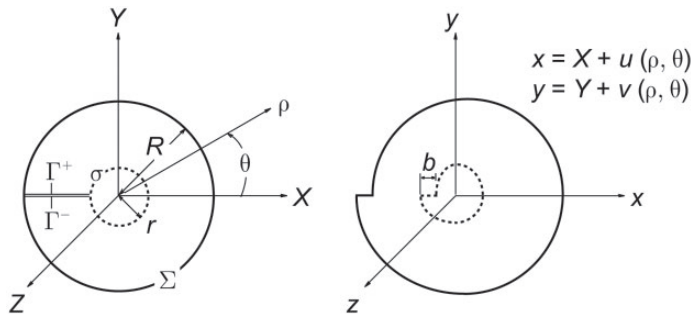


Fig. 2 Edge dislocation parallel to Z -axis centred in elastic cylinder of radius R and (out-of-plane) length L ; Burgers vector magnitude is b ; core radius is r

conditions along $Z = \pm L/2$ will lead to non-zero z -displacement w and perturbation of the other components u and v .

Often it is assumed that the cylinder is very large relative to the radial coordinate such that displacements (and stresses) vanish as $R \rightarrow \infty$ giving $a_1, a_3 \rightarrow 0$. Another frequent assumption is that effects of the traction free core can be neglected or that the radial coordinate is sufficiently larger than the core radius, leading to $r^2/\rho^2 \rightarrow 0$ and $a_2 \rightarrow 0$. When such terms corresponding to outer and core radii are omitted, strain energy per unit length e is

$$e = \frac{Gb^2}{4\pi(1-\nu)} \ln \frac{R}{r} = \bar{e} + e' = \frac{Gb^2}{12\pi} \left[\frac{1-\nu-2\nu^2}{(1-\nu)^2} \right] \ln \frac{R}{r} + \frac{Gb^2}{12\pi} \left[\frac{2-2\nu+2\nu^2}{(1-\nu)^2} \right] \ln \frac{R}{r}, \quad (3.6)$$

where G is the linear elastic shear modulus, \bar{e} is the volumetric contribution to the total line energy and e' is the deviatoric contribution.

To motivate later discussion regarding distortion, define the following surface integral:

$$\boldsymbol{\beta}_{\text{lin}}^{\text{I}} \stackrel{\text{def}}{=} \frac{1}{V} \int_{\Sigma} \mathbf{u} \otimes \mathbf{N} d\Sigma, \quad (3.7)$$

where $V = \pi R^2 L$ is the volume of the undeformed domain (including the core region) and $\mathbf{u} = u\mathbf{e}_1 + v\mathbf{e}_2 + w\mathbf{e}_3$ with $\{\mathbf{e}_i\}$ the Cartesian basis. The unit outward normal to Σ is $\mathbf{N} = \cos \theta \mathbf{e}_1 + \sin \theta \mathbf{e}_2$. Applying this definition with u from (3.3), defining $C = (1 + a_1 - a_2)|_{\rho=R}$, and noting that $d\Sigma = RLd\theta$,

$$\begin{aligned} (\beta_{12}^{\text{I}})_{\text{lin}} &= (\beta_{xy}^{\text{I}})_{\text{lin}} = \frac{1}{\pi R^2 L} \int_{\Sigma} u \sin \theta d\Sigma = \frac{1}{\pi R} \int_{-\pi}^{\pi} u \sin \theta d\theta \\ &= \frac{b}{2\pi^2 R} \int_{-\pi}^{\pi} \theta \sin \theta d\theta + \frac{b}{8(1-\nu)\pi^2 R} \int_{-\pi}^{\pi} C \sin \theta \sin 2\theta d\theta \\ &= \frac{b}{2\pi^2 R} (\sin \theta - \theta \cos \theta)|_{-\pi}^{\pi} + \frac{Cb}{48(1-\nu)\pi^2 R} (3 \sin \theta - \sin 2\theta)|_{-\pi}^{\pi} \\ &= -\frac{b}{2\pi^2 R} (\theta \cos \theta)|_{-\pi}^{\pi} = \frac{b}{\pi R}. \end{aligned} \quad (3.8)$$

It can be verified by direct integration that other planar components vanish,

$$(\beta_{11}^{\text{I}})_{\text{lin}} = \frac{1}{\pi R} \int_{-\pi}^{\pi} u \cos \theta d\theta = 0, \quad (3.9)$$

$$(\beta_{22}^{\text{I}})_{\text{lin}} = \frac{1}{\pi R} \int_{-\pi}^{\pi} v \sin \theta d\theta = 0, \quad (3.10)$$

$$(\beta_{21}^{\text{I}})_{\text{lin}} = \frac{1}{\pi R} \int_{-\pi}^{\pi} v \cos \theta d\theta = 0, \quad (3.11)$$

and since $w = 0$ and $\mathbf{N} \cdot \mathbf{e}_3 = 0$ on Σ , out-of-plane components all vanish identically: $(\beta_{13}^{\text{I}})_{\text{lin}} = (\beta_{23}^{\text{I}})_{\text{lin}} = (\beta_{31}^{\text{I}})_{\text{lin}} = (\beta_{32}^{\text{I}})_{\text{lin}} = (\beta_{33}^{\text{I}})_{\text{lin}} = 0$.

If the domain of integration is extended to include the core surface σ and the slip plane Γ^\pm , then $V_0 = \pi(R^2 - r^2)L$ is the reference volume of a simply connected domain and

$$\begin{aligned} \frac{V}{V_0} (\beta_{12}^I)_{\text{lin}} &+ \frac{1}{V_0} \int_{\sigma} u(-\sin \theta) d\sigma - \frac{1}{V_0} \int_{\Gamma^+} u d\Gamma + \frac{1}{V_0} \int_{\Gamma^-} u d\Gamma \\ &= \frac{bR}{\pi(R^2 - r^2)} - \frac{br}{\pi(R^2 - r^2)} - \frac{1}{\pi(R^2 - r^2)} \left[\frac{b}{2}(R - r) + \frac{b}{2}(R - r) \right] \\ &= \frac{b}{\pi(R + r)} - \frac{b}{\pi(R + r)} = 0, \end{aligned} \quad (3.12)$$

consistent with the proof that in the context of linear elastostatics, volume-averaged strain $\frac{1}{2V_0} \oint (\mathbf{u} \otimes \mathbf{N} + \mathbf{N} \otimes \mathbf{u}) dS = \frac{1}{2V_0} \int [\nabla \mathbf{u} + (\nabla \mathbf{u})^T] dV_0$ must vanish in a domain with uniform material properties that is in a state of self stress (that is, a homogeneous body with no traction applied to external surfaces, traction continuity across internal surfaces, and no applied body forces) (16). Summed contributions from core and slip surfaces (σ and Γ^\pm) to expressions analogous to (3.12) for other planar components of distortion also vanish.

Three-term decomposition $\mathbf{F} = \mathbf{F}^E \mathbf{F}^I \mathbf{F}^P$ of (1.2) is now revisited in the context of a volume element containing an isolated edge dislocation embedded in a larger slab of material that may contain other defects in its deformed state. Consider the cylindrical volume shown in Fig. 2, which is identified with a volume element of material to which (1.2) is applied.

The first local intermediate configuration $\tilde{\mathbf{B}}$ of this element is identified with the left part of Fig. 2: no local stress within the element or traction along its boundaries. The elastic cylinder, minus the core region, is simply connected since surfaces Γ^\pm are treated as distinct.

The second local intermediate configuration $\bar{\mathbf{B}}$ of the element is identified with the right part of Fig. 2. This element is free from traction along its external surface Σ , and thus is in a state of self stress in two dimensions (recall out-of plane stress T_{zz} is associated with the Poisson effect and plane strain). The elastic cylinder, when the core region is removed, now becomes multiply connected when referential surfaces Γ^\pm are displaced relative to one another by the Burgers vector and then bonded together. The remainder of the slab may contain defects and similar residual stresses; each element comprising the slab must, in general, be removed from its neighbours so that it too is in a state of self stress.

A local current configuration \mathbf{B} of the element is achieved when the element is stressed and deformed, along with its neighbours, so that all volume elements fit together and the body is continuous in the global current configuration. In the local current configuration for each element (not shown in Fig. 2), traction is generally non-zero on Σ .

First consider plastic deformation map \mathbf{F}^P , which accounts for n dislocations that have already moved completely through the cylinder, from left to right. Attention is restricted to edge dislocations on the single slip plane Γ , which is now extended to bisect the entire cylinder along $Y = 0$. In this case, plastic deformation is the simple shear

$$\mathbf{F}^P \stackrel{\text{def}}{=} \mathbf{1} + \gamma \mathbf{e}_1 \otimes \mathbf{e}_2, \quad (3.13)$$

where the cumulative plastic shear from relative sliding of the two sections of the cylinder is

$$\gamma \stackrel{\text{def}}{=} \sum_n \frac{1}{V} \int_0^\pi bLR \sin \theta d\theta = \frac{2bn}{\pi R}. \quad (3.14)$$

There is no plastic volume change, $J^P = \det \mathbf{F}^P = 1 + \mathbf{e}_1 \cdot \mathbf{e}_2 = 1$. Since $\mathbf{F}^{P-1} = \mathbf{1} - \gamma \mathbf{e}_1 \otimes \mathbf{e}_2$, it follows that $\dot{\mathbf{F}}^P = \dot{\mathbf{F}}^P \mathbf{F}^{P-1} = \dot{\gamma} \mathbf{e}_1 \otimes \mathbf{e}_2$. Assume for simplicity that the dislocations are equally spaced; their density is then $\zeta = 1/(\pi R^2)$. Assume also that dislocations move with constant velocity $v = 2R\dot{n}$ in the direction of \mathbf{e}_1 , where \dot{n} is the number of dislocations per unit time that transit the diameter of the cylinder; then the usual so-called Orowan equation is recovered:

$$\dot{\gamma} = \frac{2b\dot{n}}{\pi R} = \frac{bv}{\pi R^2} = \zeta bv. \quad (3.15)$$

Next consider the mapping \mathbf{F}^I . In Cartesian coordinates, this can be written

$$\mathbf{F}^I = \mathbf{1} + \boldsymbol{\beta}^I. \quad (3.16)$$

The distortion, by definition, can be further partitioned into the sum

$$\boldsymbol{\beta}^I = \boldsymbol{\beta}_{\text{lin}}^I + \boldsymbol{\beta}_{\text{nonlin}}^I + \boldsymbol{\beta}_{\text{core}}^I. \quad (3.17)$$

The linear term is defined as the distortion of the outer boundary Σ of the elastic cylinder calculated from linear elasticity, where from (3.7) and (3.8),

$$\boldsymbol{\beta}_{\text{lin}}^I = \frac{b}{\pi R} \mathbf{e}_1 \otimes \mathbf{e}_2 = \left(b^2 \zeta / \pi \right)^{1/2} \mathbf{e}_1 \otimes \mathbf{e}_2. \quad (3.18)$$

This non-symmetric term clearly includes both stretch and rotation. The other two terms are corrections accounting for non-linear elastic effects and core effects that are omitted by the linear elastic solution. Because of non-linearity, these terms in general cannot be determined exactly from superposition of solutions of decoupled boundary value problems.

The non-linear correction is defined as (17)

$$\boldsymbol{\beta}_{\text{nonlin}}^I \stackrel{\text{def}}{=} \frac{1}{V} \int_V \nabla \mathbf{u} \, dV, \quad (3.19)$$

or in indicial notation

$$\left(\boldsymbol{\beta}_{\text{nonlin}}^I \right)_{\alpha\beta} \stackrel{\text{def}}{=} \frac{1}{V} \int_V \frac{\partial u_\alpha}{\partial X_\beta} \, dV, \quad (3.20)$$

where u_α are local displacements of the self-equilibrated body in configuration \bar{B} measured from X_β , which are local coordinates in configuration \bar{B} . Let $C_{\alpha\beta\gamma\delta}$ denote the second-order elastic constants and $S_{\alpha\beta\gamma\delta}$ the complementary elastic compliance. Let $C_{\alpha\beta\gamma\delta\epsilon\zeta}$ denote third-order elastic constants, omitted in the preceding linear elastic analysis of the edge dislocation. Particular forms of elastic stiffness tensors and representative values for isotropic solids are described in Appendix A. Self-equilibrium conditions for the cylinder in configuration \bar{B} lead to vanishing of its volume averaged Cauchy stress, giving (16, 17)

$$\begin{aligned} \left(\boldsymbol{\beta}_{\text{nonlin}}^I \right)_{\mu\nu} = & -\frac{1}{V} S_{\mu\nu\alpha\beta} \left(C_{\alpha\epsilon\chi\delta} \int_V \frac{\partial u_\beta}{\partial X_\epsilon} \frac{\partial u_\chi}{\partial X_\delta} \, dV + C_{\beta\epsilon\chi\delta} \int_V \frac{\partial u_\alpha}{\partial X_\epsilon} \frac{\partial u_\chi}{\partial X_\delta} \, dV \right. \\ & \left. + \frac{1}{2} C_{\alpha\beta\chi\delta} \int_V \frac{\partial u_\epsilon}{\partial X_\chi} \frac{\partial u_\epsilon}{\partial X_\delta} \, dV + \frac{1}{2} C_{\alpha\beta\chi\delta\epsilon\phi} \int_V \frac{\partial u_\chi}{\partial X_\delta} \frac{\partial u_\epsilon}{\partial X_\phi} \, dV \right). \end{aligned} \quad (3.21)$$

to second order in displacement gradients $\nabla \mathbf{u}$, assuming elastic moduli are independent of location within V . Terms of orders three and higher in displacement gradients, involving elastic constants

of orders four and higher, are omitted. By this definition, $\boldsymbol{\beta}_{\text{nonlin}}^{\text{I}}$ is symmetric (that is, due to the symmetry of the first two components of the elastic compliance tensor); a rigid body rotation could be superposed without violating the self-equilibrium constraint. Logically, $\boldsymbol{\beta}_{\text{nonlin}}^{\text{I}}$ vanishes in the linear elastic approximation since products of order two in displacement gradients are inconsequential in the stress field of linear elasticity.

Evaluation of integral (3.21) requires knowledge of the displacement field $\mathbf{u}(\mathbf{X})$ for the non-linear elastic solution of an edge dislocation embedded in a cylinder of a third-order elastic material with finite boundaries. No known closed-form solution exists to this boundary value problem that permits ready evaluation of the integral. Zubov (18) tersely presents an exact analytical solution for an edge dislocation embedded in an infinitely extended domain of a semi-linear material; the displacement field of this solution is expressed in terms of complex functionals that cannot be easily inserted into (3.21). The stress field of the non-linear solution does, however, demonstrate significant differences from the linear elastic solution at distances up to the magnitude of several Burgers vectors from the core. Seeger et al. (19) give an approximate iterative solution for an edge dislocation accounting for up to second-order terms in displacement gradients, but the displacement field is written as a series of complex functions that do not permit analytical evaluation of (3.21). On the other hand, a tractable, yet still approximate, analytical non-linear elastic solution does exist for the screw dislocation, as will be discussed later in Section 4.

An analytical approximation for the dilatation due to non-linear elastic effects from residual stresses does exist, however, for isotropic materials as well as several cubic crystal classes. When contributions of products of orders three and higher in local displacement gradients are omitted, the volume change of an isotropic cylinder with an edge dislocation due to non-linear elasticity is (16, 17)

$$\begin{aligned} \frac{\Delta V}{V} &= \left[\frac{1}{K}(K' - 1)\bar{e} + \frac{1}{G} \left(G' - \frac{G}{K} \right) e' \right] \zeta \\ &= \frac{e}{3} \left[\frac{1 - \nu - 2\nu^2}{(1 - \nu)K} (K' - 1) + \frac{2 - 2\nu + 2\nu^2}{(1 - \nu)G} \left(G' - \frac{G}{K} \right) \right] \zeta \\ &= \left[\frac{1 - \nu - 2\nu^2}{12\pi(1 - \nu)^2} \frac{G}{K} (K' - 1) + \frac{2 - 2\nu + 2\nu^2}{12\pi(1 - \nu)^2} \left(G' - \frac{G}{K} \right) \right] b^2 \zeta \ln \frac{R}{r} = Ab^2 \zeta \ln \frac{R}{r}, \quad (3.22) \end{aligned}$$

where K is the linear elastic bulk modulus, K' and G' are pressure derivatives of the incremental bulk and shear moduli in the stress-free reference state (and can be related to third-order elastic constants as described in Appendix A), A is a constant dimensionless function of the elastic constants, and $\zeta = L/V$. In this solution, e correctly incorporates only contributions from second-order elastic constants (16), but effects of non-linearity and boundary conditions on the dislocation core and free outer radius to this contribution to elastic energy are neglected. To integral terms of at least first order in displacement gradients (17),

$$\Delta V/V \approx \det(\mathbf{1} + \boldsymbol{\beta}_{\text{nonlin}}^{\text{I}}) - 1 \approx \text{tr} \boldsymbol{\beta}_{\text{nonlin}}^{\text{I}}. \quad (3.23)$$

Knowledge of dilatation alone is insufficient to determine all components of $\boldsymbol{\beta}_{\text{nonlin}}^{\text{I}}$ resulting from an edge dislocation in an isotropic cylinder. Following (19), (15), assume that the displacement field

$$\mathbf{u} = \mathbf{u}^{(1)} + \mathbf{u}^{(2)} + \dots \approx \mathbf{u}^{(1)} + \mathbf{u}^{(2)}, \quad (3.24)$$

where $\mathbf{u}^{(1)}$ is the linear elastic solution and $\mathbf{u}^{(2)}$ is a correction that accounts for, in the resulting stress field, non-linear elastic effects of up to second order in displacement gradients. Let $\mathbf{u}^{(2)} = u^{(2)}\mathbf{e}_1 + v^{(2)}\mathbf{e}_2 + w^{(2)}\mathbf{e}_3$. Assume again that the cylinder is long (plane strain) and that the second-order correction is independent of the orientation of slip plane Γ . These symmetry arguments suggest

$$u^{(2)} = b\chi(\rho)\cos\theta, \quad v^{(2)} = b\chi(\rho)\sin\theta, \quad w^{(2)} = 0, \quad (3.25)$$

where $\chi(\rho)$ is a dimensionless correction to the radial displacement field from non-linear effects and ρ is the radial coordinate of the undeformed cylinder (left side of Fig. 2). Applying the divergence theorem,

$$\begin{aligned} (\beta_{\text{nonlin}}^{\text{I}})_{11} &\approx \frac{1}{V} \int_V \frac{\partial u^{(2)}}{\partial X} dV = \frac{1}{V} \int_{\Sigma} b\chi \cos^2 \theta d\Sigma \\ &= \frac{b}{\pi R} \chi(R) \int_{-\pi}^{\pi} \cos^2 \theta d\theta = \frac{b}{R} \chi(R), \end{aligned} \quad (3.26)$$

$$\begin{aligned} (\beta_{\text{nonlin}}^{\text{I}})_{22} &\approx \frac{1}{V} \int_V \frac{\partial v^{(2)}}{\partial Y} dV = \frac{1}{V} \int_{\Sigma} b\chi \sin^2 \theta d\Sigma \\ &= \frac{b}{\pi R} \chi(R) \int_{-\pi}^{\pi} \sin^2 \theta d\theta = \frac{b}{R} \chi(R), \end{aligned} \quad (3.27)$$

and all other terms vanish identically:

$$\begin{aligned} (\beta_{12}^{\text{I}})_{\text{nonlin}} &= (\beta_{21}^{\text{I}})_{\text{nonlin}} = (\beta_{13}^{\text{I}})_{\text{nonlin}} = (\beta_{31}^{\text{I}})_{\text{nonlin}} \\ &= (\beta_{23}^{\text{I}})_{\text{nonlin}} = (\beta_{32}^{\text{I}})_{\text{nonlin}} = (\beta_{33}^{\text{I}})_{\text{nonlin}} = 0. \end{aligned} \quad (3.28)$$

Therefore, from (3.23), a coarse approximation for the edge dislocation is

$$\chi \approx \frac{Ab}{2\pi\rho} \ln \frac{\rho}{r}, \quad (\beta_{11}^{\text{I}})_{\text{nonlin}} = (\beta_{22}^{\text{I}})_{\text{nonlin}} \approx \frac{\Delta V}{2V} \approx \frac{Ab^2}{2} \zeta \ln \frac{R}{r}. \quad (3.29)$$

Taking representative values from Table A.1 of Appendix A, (3.22) and (3.29) give $A \approx \frac{1}{12}$ and, with and $r \approx b$, $(\beta_{\text{nonlin}}^{\text{I}})_{11} = (\beta_{\text{nonlin}}^{\text{I}})_{22} \approx \frac{1}{24\pi} \frac{b^2}{R^2} \ln \frac{R}{b}$.

No analytical solution exists for $\beta_{\text{core}}^{\text{I}}$. By definition, continuum elasticity theory breaks down inside the core region, but atomic theory can be used to estimate its contribution. Term $\beta_{\text{core}}^{\text{I}}$ accounts for uncertainty in core size and shape (20) and non-zero traction imparted by the core on the surrounding continuum (15). In elastic calculations considered thus far, assumptions of a cylindrical core with minimum radius $r \approx b$ (20) imparting no traction on the surrounding material have been used. Presumably, for a small cylinder (large defect density), components of $\beta_{\text{core}}^{\text{I}}$ could be comparable or larger than those of $\beta_{\text{nonlin}}^{\text{I}}$.

In atomic simulations of an edge dislocation in α -iron (21), total dilatation was found to obey $\Delta V/V = [0.37 + 0.07 \ln(R/b)]b^2\zeta$, with contributions from non-linear and core effects estimated as similar orders of magnitude, though several arbitrary choices were made in partitioning non-linear and core contributions. In atomic simulation of the strain field of this same dislocation type

(22), it was found that deviations from the linear elastic Volterra solution could be fit to an elliptical expansion field centred slightly below the centre of the extra half-plane. The procedure for extracting residual strain fields induced by dislocation lines in atomic simulations is intricate, requiring pages of discussion in (21) too lengthy to repeat here and to which the reader is referred for details. Only their preferred end result (p. 3896 of (21) giving the just-mentioned form of $\Delta V/V$) is used in later Table 1; this result may of course be subject to possible inaccuracies associated with the numerical method of relaxation, imposition of non-unique initial conditions and boundary constraints, selection of Eulerian versus Lagrangian coordinates, choice of atomic potential, etc., noted in (21).

Three other obvious idealisations have been made in the definition of F^I . First, the linear term would be slightly different if the top and bottom faces of the cylinder were relaxed and Poisson's ratio were non-zero. Second, the dislocation is assumed centred in the cylinder. More general dislocation arrangements are mentioned in Section 5. Third, isotropic elasticity has been assumed. Anisotropic solutions would be more realistic, but general analytical solutions are not available in compact equations that are easily manipulated, except for cubic crystals of certain classes for which a solution for volume change similar to (3.22) exists (16, 17).

Combining (3.16), (3.17), (3.18), and (3.29),

$$\begin{aligned} F^I &= \mathbf{1} + \beta_{\text{lin}}^I + \beta_{\text{nonlin}}^I + \beta_{\text{core}}^I \\ &\approx \mathbf{1} + \frac{b}{\pi R} \mathbf{e}_1 \otimes \mathbf{e}_2 + \frac{A}{2\pi} \frac{b^2}{R^2} \ln \frac{R}{r} (\mathbf{e}_1 \otimes \mathbf{e}_1 + \mathbf{e}_2 \otimes \mathbf{e}_2) + \beta_{\text{core}}^I \\ &= \mathbf{1} + (b^2 \zeta / \pi)^{1/2} \mathbf{e}_1 \otimes \mathbf{e}_2 + \frac{A}{2} b^2 \zeta \ln[(\pi r^2 \zeta)^{-1/2}] (\mathbf{e}_1 \otimes \mathbf{e}_1 + \mathbf{e}_2 \otimes \mathbf{e}_2) + \beta_{\text{core}}^I. \end{aligned} \quad (3.30)$$

If the core term is omitted and the approximations $r = b$ and $A = \frac{1}{12}$ are used,

$$\beta^I = F^I - \mathbf{1} \approx (b^2 \zeta / \pi)^{1/2} \mathbf{e}_1 \otimes \mathbf{e}_2 + \frac{b^2}{24} \zeta \ln[(\pi b^2 \zeta)^{-1/2}] (\mathbf{e}_1 \otimes \mathbf{e}_1 + \mathbf{e}_2 \otimes \mathbf{e}_2). \quad (3.31)$$

Non-vanishing components of (3.31) are shown in Fig. 3, along with magnitude

$$\begin{aligned} \|\beta^I\| &= (\beta_{\alpha\beta}^I \beta_{\alpha\beta}^I)^{1/2} = \{[(\beta_{\text{lin}}^I)_{12}]^2 + 2[(\beta_{\text{nonlin}}^I)_{11}]^2 + g^2\}^{1/2} \\ &\approx \{[(b/(\pi R))]^2 + \frac{1}{288} [b/(\pi R)]^4 [\ln(R/b)]^2\}^{1/2}, \end{aligned} \quad (3.32)$$

where g is $O(\|\beta_{\text{core}}^I\|)$ and is again omitted in the final approximation. The linear contribution dominates. The theoretical maximum dislocation density is approached as $R \rightarrow R_{\text{min}} = b$ and $b^2 \zeta \rightarrow b^2 \zeta_{\text{max}} = \frac{1}{\pi}$; for example, $\zeta_{\text{max}} \approx 3 \times 10^{18} \text{m}^{-2}$ for $b^2 \approx 0.1 \text{nm}^2$. Several values are listed in Table 1. Both linear and dilatational contributions can be significant relative to applied elastic strain associated with F^E , since elastic shear strains at yielding in most crystals are on the order of $10^{-4} - 10^{-2}$. Also shown in the rightmost column of Table 1 is the normal strain (estimated as half of the total dilatation) reported from atomic simulation of a [100] edge dislocation α -iron (21). For $R/b \geq 1.7$, results of atomic calculation—which account for elastic anisotropy, elastic non-linearity and core effects—are no more than one order of magnitude larger than the third column of Table 1 that addresses isotropic non-linear elasticity alone, though generic properties from Table A.1 used in calculation of the latter are not intentionally representative of iron.

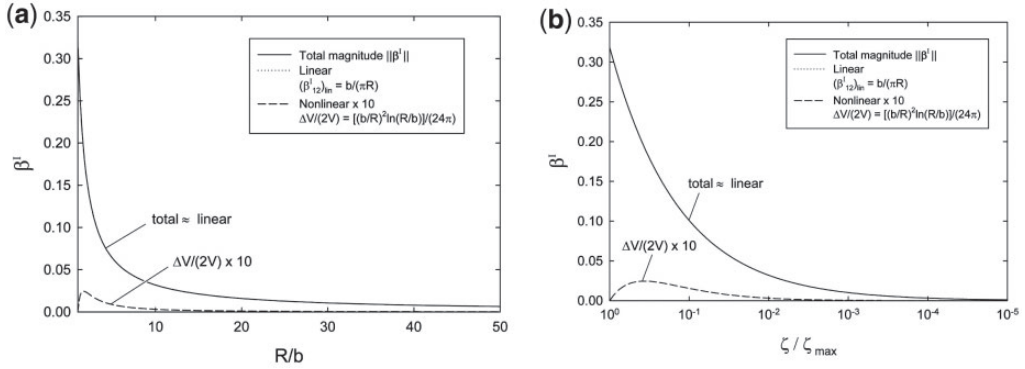


Fig. 3 Analytical estimate of shear component β^I_{12} and dilatation $\Delta V/(2V)$ for single edge dislocation centred in isotropic elastic cylinder of radius R . Normalized dislocation density is $\zeta/\zeta_{max} = b^2/R^2$

Table 1 Estimated contributions to F^I for isolated edge dislocation

R/b	ζ/ζ_{max}	$(\beta^I_{lin})_{12}$	$\Delta V/(2V)$	Atomic simulation (21)
1	1	0.32	0	5.9×10^{-2}
1.7	0.35	0.19	2.4×10^{-3}	2.3×10^{-2}
3	0.11	0.11	1.6×10^{-3}	7.8×10^{-3}
10	1.0×10^{-2}	3.2×10^{-2}	3.0×10^{-4}	8.5×10^{-4}
100	1.0×10^{-4}	3.2×10^{-3}	6.1×10^{-6}	1.1×10^{-5}

Effects of elastic anisotropy are considered in Appendix C. There it is shown that $\Delta V/(2V)$ associated with β^I_{nonlin} may be expected, due to elastic anisotropy, to increase or decrease relative to the isotropic solution by no more than a factor of around six for dislocations on typical glide systems in many Face Centred Cubic (FCC) or Body Centred Cubic (BCC) metals. Note that β^I_{lin} , which tends to dominate the magnitude of total residual lattice distortion, is unaffected by anisotropy.

From the polar decomposition theorem applied to (1.2), $F = V^E R^E F^I F^P$. Inverse stretch V^{E-1} is associated with unloading of the cylinder from its current deformed state (23), and R^E is elastic rotation that encompasses all rigid body rotation in the absence of defects. Presuming F^I and F^P are calculable from definitions given above, and that total deformation F is imposed, then $F^E = F F^{P-1} F^{I-1}$ is simply the remainder.

Several points of clarification are in order. Yielding is indicated by non-negligible plastic deformation described by F^P , which in turn depends on plastic slip γ in (3.13). For monotonic loading, $F^P = \mathbf{1}$ and $\gamma = 0$ at stresses below the yield limit. Residual lattice distortion β^I can be non-zero whenever the body contains dislocations, regardless of whether or not plastic deformation takes place concurrently (that is, regardless of whether or not dislocations are mobile). It is emphasised that F^I is not ‘plastic deformation’ but rather a kind of ‘residual elastic lattice deformation’, which justifies the summation of linear, non-linear and core elastic fields in (3.17) and (3.30). The solution for the linear elastic fields, though well known, has been included here in order to enable derivation

of $\beta_{\text{lin}}^{\text{I}}$ in a form not presented elsewhere. None of the components of β^{I} (linear, non-linear or core) can be included in F^{E} since by definitions given in Section 2, F^{E} consists of reversible or recoverable elastic deformation, while F^{I} consists of residual deformation. Instead of the summation approach in (3.17), a multiplicative split such as $F^{\text{I}} = F_{\text{lin}}^{\text{I}} F_{\text{nonlin}}^{\text{I}} F_{\text{core}}^{\text{I}}$ could be assumed. The difference between the two approaches would be $O(\|\beta^{\text{I}}\|^2)$, which a posteriori should be small relative to $\|\beta^{\text{I}}\|$ according to Table 1. Therefore, use of such a multiplicative split is not warranted at present.

4. Screw dislocation

Now consider an isolated screw dislocation of Burgers magnitude b aligned along the Z-axis, contained within a cylinder of the same geometry as shown on the left side of Fig. 2. Boundaries of the outside of the cylinder and the core are Σ and σ , and Γ^+ and Γ^- are boundaries of the slip plane along $\{X, 0^+, Z\}$ and $\{X, 0^-, Z\}$ for $-R \leq X \leq -r$. Let

$$b = z(\rho, \pi) - z(\rho, -\pi), \quad R \geq \rho \geq r. \quad (4.1)$$

Let the resultant force and torque on each end of the cylinder at $Z = \pm L/2$ vanish. In physical components, the displacement field for the linear solution is (15)

$$u_\theta = -\frac{b\rho Z}{\pi R^2}, \quad u_z = w = \frac{b\theta}{2\pi}. \quad (4.2)$$

The analogue of (3.6), for $L \rightarrow \infty$, is

$$e = e' = \frac{Gb^2}{4\pi} \ln \frac{R}{r}, \quad \bar{e} = 0. \quad (4.3)$$

Applying definition (3.7) for this isolated screw dislocation,

$$\begin{aligned} (\beta_{32}^{\text{I}})_{\text{lin}} &= (\beta_{zY}^{\text{I}})_{\text{lin}} = \frac{1}{\pi R^2 L} \int_{\Sigma} w \sin \theta d\Sigma = \frac{1}{\pi R} \int_{-\pi}^{\pi} w \sin \theta d\theta \\ &= \frac{b}{2\pi^2 R} \int_{-\pi}^{\pi} \theta \sin \theta d\theta = \frac{b}{2\pi^2 R} (\sin \theta - \theta \cos \theta)|_{-\pi}^{\pi} = \frac{b}{\pi R}. \end{aligned} \quad (4.4)$$

All other components vanish:

$$\begin{aligned} (\beta_{11}^{\text{I}})_{\text{lin}} &= (\beta_{12}^{\text{I}})_{\text{lin}} = (\beta_{13}^{\text{I}})_{\text{lin}} = (\beta_{21}^{\text{I}})_{\text{lin}} = (\beta_{22}^{\text{I}})_{\text{lin}} \\ &= (\beta_{23}^{\text{I}})_{\text{lin}} = (\beta_{31}^{\text{I}})_{\text{lin}} = (\beta_{33}^{\text{I}})_{\text{lin}} = 0. \end{aligned} \quad (4.5)$$

Three-term decomposition $F = F^{\text{E}} F^{\text{I}} F^{\text{P}}$ of (1.2) is now revisited in the context of a volume element containing an isolated screw dislocation embedded in a larger slab of material that may contain other defects in its deformed state.

First consider plastic deformation map F^{P} , which accounts for n dislocations that have already moved completely through the cylinder. Attention is restricted to screw dislocations on the single

slip plane Γ , which is now extended to bisect the entire cylinder along its axis. In this case, plastic deformation is the simple shear

$$\mathbf{F}^P \stackrel{\text{def}}{=} \mathbf{1} + \gamma \mathbf{e}_3 \otimes \mathbf{e}_2, \quad (4.6)$$

where the cumulative plastic shear from relative sliding of the two sections of the cylinder is

$$\gamma \stackrel{\text{def}}{=} \sum_n \frac{1}{V} \int_0^\pi bLR \sin \theta d\theta = \frac{2bn}{\pi R}. \quad (4.7)$$

There is no plastic volume change: $J^P = \det \mathbf{F}^P = 1 + \mathbf{e}_3 \cdot \mathbf{e}_2 = 1$. Assume for simplicity that the dislocations are equally spaced; their density is then $\zeta = \frac{1}{\pi R^2}$. Assume also that dislocations move with constant velocity $v = 2R\dot{n}$; then

$$\dot{\gamma} = \frac{2b\dot{n}}{\pi R} = \frac{bv}{\pi R^2} = \zeta bv. \quad (4.8)$$

Equations (4.7) and (4.8) are identical to (3.14) and (3.15), respectively.

Next consider the mapping \mathbf{F}^I . Equations (3.16) and (3.17) still apply. The linear contribution is

$$\boldsymbol{\beta}_{\text{lin}}^I = \frac{b}{\pi R} \mathbf{e}_3 \otimes \mathbf{e}_2 = \left(b^2 \zeta / \pi \right)^{1/2} \mathbf{e}_3 \otimes \mathbf{e}_2, \quad (4.9)$$

which includes both stretch and rotation. The non-linear correction is defined as in (3.19), (3.20) and (3.21). When contributions of products of orders three and higher in local displacement gradients are omitted, the volume change of an isotropic cylinder with a screw dislocation due to non-linear elastic effects is **(16, 17)**

$$\frac{\Delta V}{V} = \frac{e}{G} \left(G' - \frac{G}{K} \right) \zeta = \frac{1}{4\pi} \left(G' - \frac{G}{K} \right) b^2 \zeta \ln \frac{R}{r} = Ab^2 \zeta \ln \frac{R}{r}, \quad (4.10)$$

where A is a different constant dimensionless function of the elastic constants, and $\zeta = L/V$. Taking values from Table A.1 as representative, $A \approx \frac{1}{32}$. In this solution, $e = e'$ correctly incorporates only contributions from second-order elastic constants **(16)**, but effects of nonlinearity and boundary conditions on the dislocation core and free outer radius to this contribution to elastic energy are neglected.

Knowledge of the dilatation alone is insufficient to determine all components of $\boldsymbol{\beta}_{\text{nonlin}}^I$ resulting from a screw dislocation in an isotropic cylinder. Evaluation of integral (3.21) requires knowledge of the displacement field $\mathbf{u}(\mathbf{X})$ for the non-linear elastic solution of a screw dislocation embedded in a cylinder of a third-order elastic material with finite boundaries. No known exact closed-form solution exists to this boundary value problem that permits ready evaluation of the integral. Zubov **(24)** presents an exact analytical solution for a screw dislocation embedded in an incompressible non-linear elastic material. The stress field of this non-linear solution demonstrates significant differences from the linear elastic solution as $\rho \rightarrow b$. The incompressibility constraint ($\nu \rightarrow 0.5$) is not realistic for most crystals and precludes calculation of dilatation due to geometric and material nonlinearity. Teodosiu **(15)** gives an approximate iterative solution for a screw dislocation embedded in a cylindrical domain accounting for up to second-order terms in displacement gradients, where the cylinder is infinitely long but may have free boundaries at r and R . This solution will be used to

inform (3.21) in what follows. Earlier, Willis (25) obtained a similar, but not identical, approximate solution for a screw dislocation in an infinite medium using Green's functions.

Following (15) (p. 211), assume that (3.24) holds, where $\mathbf{u}^{(1)}$ is the linear elastic solution and $\mathbf{u}^{(2)}$ is a correction that accounts for, in the resulting stress field, non-linear elastic effects of up to second order in displacement gradients. Let $\mathbf{u}^{(2)} = u^{(2)}\mathbf{e}_1 + v^{(2)}\mathbf{e}_2 + w^{(2)}\mathbf{e}_3$. The approximate non-linear solution is of the form

$$u^{(2)} = \eta(\rho) \cos \theta, \quad v^{(2)} = \eta(\rho) \sin \theta, \quad w^{(2)} = 0, \quad (4.11)$$

where $\eta(\rho)$ is a correction to the radial displacement field from non-linear effects, and ρ is the radial coordinate of the dislocated cylinder. When the core surface at $\rho = r$ is traction-free, the solution is (15) (p. 231)

$$\eta(\rho) = \frac{c_1}{\rho} + c_2\rho + c_3 \frac{\ln \rho}{\rho}, \quad (4.12)$$

where c_1 , c_2 and c_3 depend on b , r , R , and the second- and third-order elastic constants, and are given in Appendix B. Applying the divergence theorem,

$$\begin{aligned} (\beta_{\text{nonlin}}^{\text{I}})_{\alpha\beta} &\approx \frac{1}{V} \int_V \frac{\partial u_\alpha^{(2)}}{\partial X_\beta} dV = \frac{1}{V} \int_\Sigma u_\alpha^{(2)} N_\beta d\Sigma \\ &= \frac{1}{\pi [R - \eta(R)]^2} \int_{-\pi}^{\pi} u_\alpha^{(2)} N_\beta [R - \eta(R)] d\theta, \end{aligned} \quad (4.13)$$

where the Lagrangian radial coordinate of Σ is $R - \eta(R)$, since ρ is the Eulerian radial coordinate in the solution of (15). Non-vanishing components of (4.13) are

$$(\beta_{\text{nonlin}}^{\text{I}})_{11} \approx \frac{1}{\pi [R - \eta(R)]} \int_{-\pi}^{\pi} \eta(R) \cos^2 \theta d\theta = \frac{\eta(R)}{R - \eta(R)}, \quad (4.14)$$

$$(\beta_{\text{nonlin}}^{\text{I}})_{22} \approx \frac{1}{\pi [R - \eta(R)]} \int_{-\pi}^{\pi} \eta(R) \sin^2 \theta d\theta = \frac{\eta(R)}{R - \eta(R)}; \quad (4.15)$$

all other terms vanish identically, that is, (3.28) applies for the screw dislocation.

Combining (3.16), (3.17), (4.4), (4.14) and (4.15),

$$\begin{aligned} \mathbf{F}^{\text{I}} &= \mathbf{1} + \boldsymbol{\beta}_{\text{lin}}^{\text{I}} + \boldsymbol{\beta}_{\text{nonlin}}^{\text{I}} + \boldsymbol{\beta}_{\text{core}}^{\text{I}} \\ &\approx \mathbf{1} + \frac{b}{\pi R} \mathbf{e}_3 \otimes \mathbf{e}_2 + \frac{\eta(R)}{R - \eta(R)} (\mathbf{e}_1 \otimes \mathbf{e}_1 + \mathbf{e}_2 \otimes \mathbf{e}_2) + \boldsymbol{\beta}_{\text{core}}^{\text{I}} \\ &= \mathbf{1} + (b^2 \zeta / \pi)^{1/2} \mathbf{e}_3 \otimes \mathbf{e}_2 + \frac{\eta[(\pi \zeta)^{-1/2}]}{(\pi \zeta)^{-1/2} - \eta[(\pi \zeta)^{-1/2}]} (\mathbf{e}_1 \otimes \mathbf{e}_1 + \mathbf{e}_2 \otimes \mathbf{e}_2) + \boldsymbol{\beta}_{\text{core}}^{\text{I}}. \end{aligned} \quad (4.16)$$

Calculable terms of (4.16) and dilatation $\Delta V / (2V)$ from (4.10) are compared in Fig. 4, along with the magnitude

$$\begin{aligned} \|\boldsymbol{\beta}^{\text{I}}\| &= (\beta_{\alpha\beta}^{\text{I}} \beta_{\alpha\beta}^{\text{I}})^{1/2} = \{[(\beta_{\text{lin}}^{\text{I}})_{32}]^2 + f^2 + g^2\}^{1/2} \\ &\approx \{[(b/(\pi R))]^2 + 2[(\beta_{\text{nonlin}}^{\text{I}})_{11}]^2\}^{1/2}, \end{aligned} \quad (4.17)$$

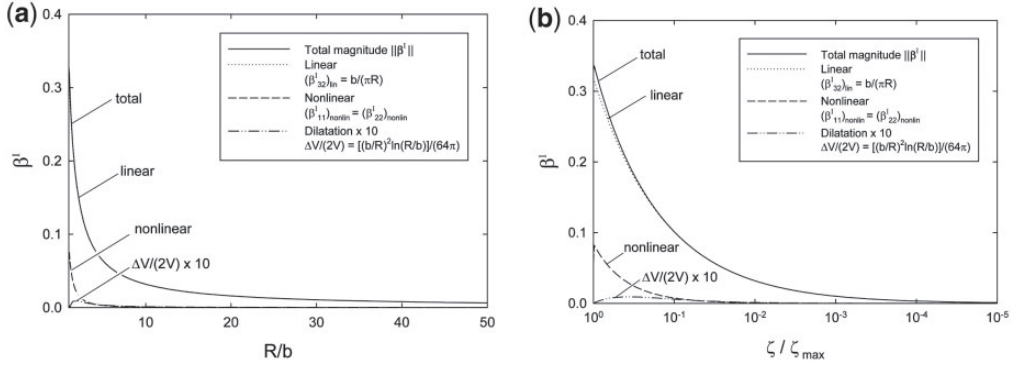


Fig. 4 Analytical estimate of shear component β_{32}^I , non-linear contribution $\beta_{11}^I = \beta_{22}^I$, and dilatation $\Delta V/(2V)$ for single screw dislocation centred in isotropic elastic cylinder of radius R . Normalised dislocation density is $\zeta/\zeta_{\max} = b^2/R^2$. In part (a), total and linear curves are visibly indistinguishable.

Table 2 Estimated contributions to F^I for isolated screw dislocation.

R/b	ζ/ζ_{\max}	$(\beta_{\text{lin}}^I)_{32}$	$(\beta_{\text{nonlin}}^I)_{11}$	$\Delta V/(2V)$	$(\beta_{\text{core}}^I)_{11} \cdot G/\hat{p}$
1	1	0.32	5.9×10^{-2}	0	∞
1.7	0.35	0.19	2.7×10^{-2}	9.1×10^{-4}	0.40
3	0.11	0.11	8.2×10^{-3}	6.1×10^{-4}	9.3×10^{-2}
10	1.0×10^{-2}	3.2×10^{-2}	7.0×10^{-4}	1.2×10^{-4}	7.6×10^{-3}
100	1.0×10^{-4}	3.2×10^{-3}	6.2×10^{-6}	2.3×10^{-6}	7.5×10^{-5}

where $f = \sqrt{2}(\beta_{\text{nonlin}}^I)_{11} = \sqrt{2}(\beta_{\text{nonlin}}^I)_{22}$ is the non-linear elastic contribution, and g is $O(\|\beta_{\text{core}}^I\|)$ and is omitted in the final approximation. In the context of (4.19) and (4.20) to be discussed later, $g = \sqrt{2}(\beta_{\text{core}}^I)_{11} = \sqrt{2}(\beta_{\text{core}}^I)_{22} \propto \hat{p}/G$ and increases with increasing ζ , with \hat{p} radial pressure exerted by the core on the surrounding crystal. The linear term exceeds f , though the latter is not insignificant. Several values are listed in Table 2. Linear, non-linear and core contributions can all be substantial relative to applied elastic strain associated with F^E .

Note that an approximation of the non-linear contribution in terms of dilatation such as that made in (3.29) is not necessary for the screw dislocation since the second-order non-linear elastic solution for η is available for this geometry. As is clear from Table 2, non-linear term $(\beta_{\text{nonlin}}^I)_{11}$ exceeds dilatational term $\Delta V/(2V)$ by several orders of magnitude near the theoretical maximum density, but both terms are of comparable magnitude for $\zeta/\zeta_{\max} \leq 0.01$. The former is presumably more accurate because it accounts consistently for non-linear contributions to the elastic energy of the dislocation and the free boundary at $\rho = R$; however, it is still an approximation because non-linear contributions to the average axial stress need not vanish (the cylinder is not self-equilibrated in the axial direction). The latter approximation (dilatation) relies on elastic energy per unit length of a screw dislocation in an infinite linear elastic medium. Both approximations $[(\beta_{\text{nonlin}}^I)_{11}$ and $\Delta V/(2V)]$ omit higher-order corrections involving contributions of terms of order three and higher in local displacement gradients to stresses and average strains, and both also neglect contributions of the dislocation core to traction at $\rho = r$. For values of material constants considered here, both approximations do however

demonstrate positive volume change that has been confirmed experimentally for cold-worked metals with cubic symmetry (26).

Now consider $\beta_{\text{core}}^{\text{I}}$. As for the edge dislocation, continuum elasticity theory cannot be applied to describe the core of a screw dislocation, and $\beta_{\text{core}}^{\text{I}}$ accounts for uncertainty in core size and shape and non-zero traction imparted by the core on the surrounding crystal. In an isotropic linear elastic solid, the contribution of a radial pressure \hat{p} acting on core surface $\rho = r$ to the dilatation of the solid can be determined analytically. Displacement \hat{u} imparted by such a core pressure is radial (15):

$$\hat{u}(\rho) = \frac{\hat{p}r^2}{2G(R^2 - r^2)} \left[(1 - 2\nu)\rho + \frac{R^2}{\rho} \right]. \quad (4.18)$$

Non-zero components of $\beta_{\text{core}}^{\text{I}}$ then follow as

$$(\beta_{\text{core}}^{\text{I}})_{11} \approx \frac{1}{\pi R} \int_{-\pi}^{\pi} \hat{u} \cos^2 \theta d\theta = \frac{(1 - \nu)\hat{p}}{G} \frac{r^2}{R^2 - r^2} = \frac{(1 - \nu)\hat{p}}{G} \frac{\zeta/\zeta_{\text{max}}}{1 - \zeta/\zeta_{\text{max}}}, \quad (4.19)$$

$$(\beta_{\text{core}}^{\text{I}})_{22} \approx \frac{1}{\pi R} \int_{-\pi}^{\pi} \hat{u} \sin^2 \theta d\theta = \frac{(1 - \nu)\hat{p}}{G} \frac{r^2}{R^2 - r^2} = \frac{(1 - \nu)\hat{p}}{G} \frac{\zeta/\zeta_{\text{max}}}{1 - \zeta/\zeta_{\text{max}}}. \quad (4.20)$$

Predicted components of $\beta_{\text{core}}^{\text{I}}$ can be comparable or larger than those of $\beta_{\text{nonlin}}^{\text{I}}$, and the core contribution becomes singular as the cylinder shrinks to the core itself ($R/b \rightarrow 1$). Representative values are listed in Table 2 for $r = b$ and $\nu = \frac{1}{4}$. Core pressure \hat{p} at a prescribed radius r must be supplied by atomic theory; recent calculations for dislocations in aluminum (27) suggest that $|\hat{p}| \lesssim 0.1G$. At $\hat{p}/G = \frac{1}{10}$, $\beta_{\text{core}}^{\text{I}} \approx \beta_{\text{nonlin}}^{\text{I}}$ for $R \geq 1.7b$. At very large pressures (for example, \hat{p} approaching G) the linear elastic estimate of $\beta_{\text{core}}^{\text{I}}$ in (4.19) and (4.20) would not be expected to be accurate, and non-zero core traction would also alter the solution in Appendix B and Table 2 for the non-linear elastic contribution to dilatation. Density functional theory calculations (28) for core contributions to displacements for various [111] screw dislocation dipole arrangements in α -iron predict dilatation perpendicular to the dislocation line and contraction, smaller in magnitude, parallel to the line. These calculations incorporate relaxed periodic boundary conditions, while the elastic solutions used herein for screw dislocations omit the possibility of deformation parallel to the infinitely extended dislocation line.

The same comments regarding the polar decomposition of F^{E} near the end of Section 3 apply for the isolated screw dislocation.

5. Generalisations

5.1 Multiple and moving dislocations

Since F^{I} and F^{P} are not state functions but instead depend on load history for arbitrary deformation paths, it is most appropriate to consider rate forms of these quantities for generalisation to an element of a single crystal with multiple dislocations whose number and position change with time. Let the total velocity gradient

$$\mathbf{L} \stackrel{\text{def}}{=} \dot{\mathbf{F}}\mathbf{F}^{-1} = \dot{\mathbf{F}}^{\text{E}}\mathbf{F}^{\text{E}-1} + \mathbf{F}^{\text{E}}\mathbf{F}^{\text{I}}(\mathbf{L}^{\text{I}} + \mathbf{L}^{\text{P}})\mathbf{F}^{\text{I}-1}\mathbf{F}^{\text{E}-1}; \quad (5.1)$$

$$\mathbf{L}^{\text{I}} \stackrel{\text{def}}{=} \mathbf{F}^{\text{I}-1}\dot{\mathbf{F}}^{\text{I}}, \quad \mathbf{L}^{\text{P}} \stackrel{\text{def}}{=} \dot{\mathbf{F}}^{\text{P}}\mathbf{F}^{\text{P}-1}. \quad (5.2)$$

Superposed dots denote material time derivatives, d/dt . Both L^I and L^P have components referred to the same intermediate configuration \tilde{B} introduced in Section 2.

Consider a single crystal with one or more glide systems labelled by index k . Let $\zeta^{(k)} \geq 0$ denote the line length per unit reference volume of dislocations associated with system k , and let $\mathbf{b}^{(k)}$ and $\mathbf{m}^{(k)}$ denote the associated Burgers vector and unit normal to the slip plane in the undeformed perfect crystal. Restricting attention to slip systems with the same Burgers magnitude, let $\mathbf{b}^{(k)} = b\mathbf{s}^{(k)}$, where $\mathbf{s}^{(k)}$ is a unit vector in the direction of slip in the perfect reference lattice. Associate a uniform velocity $v^{(k)}$ with each dislocation population; immobile dislocations have $v^{(k)} = 0$. Edge, screw and mixed dislocations and loops can contribute to the same or different densities $\zeta^{(k)}$ depending on their velocities and Burgers vectors. Generalisation of (3.13)–(3.15) and (4.6)–(4.8) to multiple slip systems leads to the usual rate kinematics of continuum crystal plasticity theory:

$$L^P = \sum_k \zeta^{(k)} v^{(k)} \mathbf{b}^{(k)} \otimes \mathbf{m}^{(k)} = \sum_k \dot{\gamma}^{(k)} \mathbf{s}^{(k)} \otimes \mathbf{m}^{(k)}. \quad (5.3)$$

Now consider F^I generalised to a volume element containing multiple dislocations of various orientations and various edge and screw components. Motivated by developments in Sections 3 and 4, the linear contribution to F^I depends on the path each dislocation has traveled through the volume element. The magnitude of each dislocation's contribution to β_{lin}^I is proportional to its slipped distance through the volume element under consideration. For example, an edge dislocation that has traveled almost completely across a cylinder as in Section 3 would contribute $(\beta_{\text{lin}}^I)_{12} \rightarrow \frac{2b}{\pi R}$ as the slipped distance $\rightarrow 2R$. It is assumed here that the contributions of all dislocations comprising a given family k are equivalent to those of a density $\zeta^{(k)}$ located at the centre of the volume element, such that, from generalisation of (3.18) and (4.9),

$$L_{\text{lin}}^I = \sum_k \frac{d}{dt} [(b^2 \zeta^{(k)} / \pi)^{1/2}] \mathbf{s}^{(k)} \otimes \mathbf{m}^{(k)} = \frac{1}{2\sqrt{\pi}} \sum_k [\dot{\zeta}^{(k)} (\zeta^{(k)})^{-1/2}] \mathbf{b}^{(k)} \otimes \mathbf{m}^{(k)}. \quad (5.4)$$

The factor $\frac{1}{2\sqrt{\pi}}$ is replaced by $\frac{1}{2\sqrt{2}}$ if a hexahedral volume element with equal edge lengths is considered instead of a cylinder. Dislocations with parallel Burgers vectors of equal length but opposite sign must be assigned to distinct populations $\zeta^{(k)}$ with parallel but oppositely signed directions $\mathbf{s}^{(k)}$ (for example, 24 populations for conventional $\{111\}\langle 110\rangle$ slip in FCC crystals). With this convention, $v^{(k)} \geq 0$ and $\dot{\gamma}^{(k)} \geq 0$ can be enforced. A slightly different form for the strain rate contribution from dislocation generation (dislocation density rate distinct from slip) has been proposed elsewhere for shock compressed polycrystalline metals (29).

The non-linear contribution to F^I is independent of the path of dislocation motion (the orientation of the glide plane and the slipped distance), and depends only on the number, orientation and location of dislocations within the element. For single slip ($k = 1$) of edge dislocations, straightforward generalisation of (3.29) leads to

$$L_{\text{nonlin}}^I \approx \dot{\beta}_{\text{nonlin}}^I = -\frac{Ab^2}{4} [\ln(\pi b^2 \zeta) + 1] \dot{\zeta} (\mathbf{s} \otimes \mathbf{s} + \mathbf{m} \otimes \mathbf{m}), \quad (5.5)$$

where A is defined in (3.22) and depends on linear and non-linear elastic properties. A similar approach with (4.14) and (4.15) could be used for a single system of screw dislocations. An analytical non-linear solution to (3.21) is not available for dislocation networks often formed under

activity of multiple interacting slip systems; non-linear solutions for even isolated dislocations are scarce and approximate as mentioned already. Motivated by forms of $\boldsymbol{\beta}_{\text{nonlin}}^{\text{I}}$ for isolated edge and screw dislocations in Sections 3 and 4, as a further approximation it could be assumed that each dislocation line contributes a radial deformation (a radial expansion or dilatation for material properties considered herein). For many dislocation lines of various orientations, the net contribution would then be approximated as a pure volume change:

$$\boldsymbol{\beta}_{\text{nonlin}}^{\text{I}} \approx \varphi(\zeta^{(k)})\mathbf{1} = \varphi(\zeta^{(k)})\mathbf{e}_\alpha \otimes \mathbf{e}_\alpha, \quad (5.6)$$

where φ is a dimensionless scalar function of dislocation densities. Letting $\zeta = \sum_k \zeta^{(k)}$,

$$\varphi|_{\zeta=0} = 0, \quad \varphi|_{\zeta \rightarrow \zeta_{\text{max}}} \approx 0.001 - 0.1, \quad (5.7)$$

where the estimated magnitude at maximum dislocation density is motivated by Tables 1 and 2 and therefore applies for a representative crystalline material with properties in Table A.1. Then

$$\mathbf{L}_{\text{nonlin}}^{\text{I}} \approx \dot{\boldsymbol{\beta}}_{\text{nonlin}}^{\text{I}} = \dot{\varphi}\mathbf{1} = \sum_k \frac{\partial \varphi}{\partial \zeta^{(k)}} \dot{\zeta}^{(k)}\mathbf{1}. \quad (5.8)$$

A dilatational contribution to total deformation has been confirmed experimentally for several metals (26). Highly structured anisotropic dislocation arrangements, such as those occurring in dislocation cell walls, would presumably also give a deviatoric contribution to $\mathbf{L}_{\text{nonlin}}^{\text{I}}$, but an analytical form for such contributions remains undetermined. Combining (5.4) and (5.8) and adding a core contribution as in (3.17),

$$\mathbf{L}^{\text{I}} = \mathbf{L}_{\text{lin}}^{\text{I}} + \mathbf{L}_{\text{nonlin}}^{\text{I}} + \mathbf{L}_{\text{core}}^{\text{I}}, \quad (5.9)$$

where $\mathbf{L}_{\text{lin}}^{\text{I}}$ is deviatoric (traceless) from (5.4), $\mathbf{L}_{\text{nonlin}}^{\text{I}}$ is estimated as spherical (diagonal) in (5.8) (30), and $\mathbf{L}_{\text{core}}^{\text{I}} \approx \dot{\boldsymbol{\beta}}_{\text{core}}^{\text{I}}$ must be determined from atomic theory. The particular form of the latter is unknown from the present non-linear elastic analysis, but $\boldsymbol{\beta}_{\text{core}}^{\text{I}}$ must vanish when $\zeta = 0$ and presumably $\mathbf{L}_{\text{core}}^{\text{I}}$ depends on $\dot{\zeta}^{(k)}$. For an isotropic uniform distribution of screw dislocations, $\mathbf{L}_{\text{core}}^{\text{I}}$ could be estimated by time differentiation of (4.19) and (4.20), but such an approach would not be valid for edge dislocations or anisotropic solids, since atomic calculations (22) show that the core contribution is not spherical.

The total velocity gradient of (5.1) can now be written

$$\mathbf{L} = \dot{\mathbf{F}}^{\text{E}}\mathbf{F}^{\text{E}-1} + \sum_k b\zeta^{(k)} \left[\mathbf{v}^{(k)} + \frac{1}{2\sqrt{\pi}} \{ \dot{\zeta}^{(k)} (\zeta^{(k)})^{-3/2} \} \right] \hat{\mathbf{s}}^{(k)} \otimes \hat{\mathbf{m}}^{(k)} + \sum_k \frac{\partial \varphi}{\partial \zeta^{(k)}} \dot{\zeta}^{(k)}\mathbf{1} + \hat{\mathbf{L}}_{\text{core}}^{\text{I}}, \quad (5.10)$$

where quantities pushed forward by the total (recoverable + residual) lattice deformation are

$$\hat{\mathbf{s}}^{(k)} \stackrel{\text{def}}{=} \mathbf{F}^{\text{E}}\mathbf{F}^{\text{I}}\mathbf{s}^{(k)}, \quad \hat{\mathbf{m}}^{(k)} \stackrel{\text{def}}{=} (\mathbf{F}^{\text{E}}\mathbf{F}^{\text{I}})^{-\text{T}}\mathbf{m}^{(k)}, \quad \hat{\mathbf{L}}_{\text{core}}^{\text{I}} \stackrel{\text{def}}{=} \mathbf{F}^{\text{E}}\mathbf{F}^{\text{I}}\mathbf{L}_{\text{core}}^{\text{I}}\mathbf{F}^{\text{I}-1}\mathbf{F}^{\text{E}-1}. \quad (5.11)$$

The total velocity gradient contains contributions from elasticity, dislocation motion (\mathbf{L}^{P}) and dislocation generation (\mathbf{L}^{J}). Notice that

$$\mathbf{v}^{(k)} = 0(\forall k) \Rightarrow \mathbf{L}^{\text{P}} = 0, \quad \dot{\zeta}^{(k)} = 0(\forall k) \Rightarrow \mathbf{L}^{\text{J}} = 0; \quad (5.12)$$

$$\zeta^{(k)} = 0(\forall k) \Rightarrow \mathbf{L}^{\text{P}} = 0 \quad \text{and} \quad \mathbf{F}^{\text{I}} = \mathbf{1}. \quad (5.13)$$

Elastic part $\dot{\mathbf{F}}^E \mathbf{F}^{E-1}$ is the remainder if \mathbf{L} is imposed, and is associated with rigid spin and the rate of stress applied to the element's boundaries.

5.2 Energy in constitutive models of crystals with defects

Let $\boldsymbol{\epsilon}$ be a frame indifferent measure of finite elastic strain, for example,

$$\boldsymbol{\epsilon} = \frac{1}{2}(\mathbf{F}^{ET} \mathbf{F}^E - \mathbf{1}), \quad \epsilon_{\alpha\beta} = \frac{1}{2}(F_{i\alpha}^E F_{i\beta}^E - \delta_{\alpha\beta}). \quad (5.14)$$

Let ξ be a dimensionless internal state variable accounting for effects of dislocations on energy density, for example,

$$\xi = b\zeta^{1/2} = b \left(\sum_k \zeta^{(k)} \right)^{1/2}. \quad (5.15)$$

Total strain energy (free energy omitting temperature dependence) per unit volume in configuration B_0 for an element of crystalline material with dislocations is posited as

$$\Psi = \Psi(\boldsymbol{\epsilon}, \xi) = W(\boldsymbol{\epsilon}) + \iota(\xi) + \psi(\boldsymbol{\epsilon}, \xi). \quad (5.16)$$

Letting $(\)|_0$ denote a quantity evaluated at the reference state wherein $\boldsymbol{\epsilon} = 0$ and $\xi = 0$, a series expansion is

$$W = \frac{1}{2} \frac{\partial^2 W}{\partial \epsilon_{\alpha\beta} \partial \epsilon_{\gamma\delta}} \Big|_0 \epsilon_{\alpha\beta} \epsilon_{\gamma\delta} + \frac{1}{6} \frac{\partial^3 W}{\partial \epsilon_{\alpha\beta} \partial \epsilon_{\gamma\delta} \partial \epsilon_{\epsilon\phi}} \Big|_0 \epsilon_{\alpha\beta} \epsilon_{\gamma\delta} \epsilon_{\epsilon\phi} + \dots, \quad (5.17)$$

$$\iota = \frac{1}{2} \frac{\partial^2 \iota}{\partial \xi^2} \Big|_0 \xi^2 + \frac{1}{6} \frac{\partial^3 \iota}{\partial \xi^3} \Big|_0 \xi^3 + \dots, \quad (5.18)$$

$$\psi = \frac{\partial^2 \psi}{\partial \epsilon_{\alpha\beta} \partial \xi} \Big|_0 \epsilon_{\alpha\beta} \xi + \frac{1}{2} \frac{\partial^3 \psi}{\partial \epsilon_{\alpha\beta} \partial \xi^2} \Big|_0 \epsilon_{\alpha\beta} \xi^2 + \frac{1}{2} \frac{\partial^3 \psi}{\partial \epsilon_{\alpha\beta} \partial \epsilon_{\gamma\delta} \partial \xi} \Big|_0 \epsilon_{\alpha\beta} \epsilon_{\gamma\delta} \xi + \dots, \quad (5.19)$$

where constant and linear terms in strain or defect density are eliminated so that conjugate thermodynamic forces vanish in the reference state. Coefficients of strain in elastic energy W are second-, third-, ...order elastic constants for a perfect crystal (see Appendix A). Function ι accounts for self-energy of dislocations within the externally unloaded (self-equilibrated) volume element, including local elastic self-energy, core energy and interaction energies (31) among dislocations within the element (longer range or inter-element dislocation interactions are measured by $\boldsymbol{\epsilon}$). Function ψ accounts for coupling between applied loading and defects, and while usually omitted in constitutive models, should not be arbitrarily dismissed when defect density approaches its theoretical maximum. For example, the third term on the right in (5.19) accounts for influence of defects on tangent elastic coefficients (32).

Term \mathbf{F}^I is not included explicitly in (5.16) since it is assumed that contributions from defects are fully represented by ξ . However, $\xi = b\sqrt{\zeta}$ and \mathbf{F}^I or its spatial gradient are not necessarily independent. Let $\zeta = \zeta(\boldsymbol{\zeta}^G, \zeta^S)$, where $\boldsymbol{\zeta}^G$ and ζ^S are the tensor density of geometrically necessary dislocations and scalar density of statistically stored dislocations, the latter having no net Burgers

vector. In the theory of continuously distributed dislocations, ζ^G contained in a local volume element is related to that element's plastic curvature (15, 25, 33):

$$\zeta^G \stackrel{\text{def}}{=} J^{P-1} \mathbf{F}^P (\nabla \times \mathbf{F}^P), \quad \zeta_{\alpha\beta}^G \stackrel{\text{def}}{=} J^{P-1} F_{\alpha I}^P e_{IJK} \partial_J F_{\beta K}^P, \quad (5.20)$$

where $J^P = \det \mathbf{F}^P = 1$ and ∇ is the material gradient in the present context, e_{IJK} are permutation symbols, and the algebraic sign convention and order of indices in ζ^G varies in the literature (1, 2, 25, 33). It can be shown that (34)

$$J^{P-1} F_{\alpha I}^P e_{IJK} \partial_J F_{\beta K}^P = J^E J^I F_{\alpha\delta}^{I-1} F_{\delta i}^{E-1} e_{ijk} \partial_j (F_{\beta\gamma}^{I-1} F_{\gamma k}^{E-1}). \quad (5.21)$$

Though not necessary, if \mathbf{F}^{E-1} obeys integrability conditions $\partial_k F_{\alpha i}^{E-1} = \partial_i F_{\alpha k}^{E-1}$, then

$$\zeta_{\alpha\beta}^G = J^E J^I F_{\alpha\delta}^{I-1} F_{\delta i}^{E-1} F_{\gamma k}^{E-1} e_{ijk} \partial_j F_{\beta\gamma}^{I-1}, \quad (5.22)$$

which implies $\xi = \xi(\zeta^S, \mathbf{F}^E, \mathbf{F}^I, \nabla \mathbf{F}^I)$ with ∇ here the spatial gradient, and thus

$$\Psi = \Psi(\boldsymbol{\epsilon}, \xi) \rightsquigarrow \Psi = \Psi(\mathbf{F}^E, \mathbf{F}^I, \nabla \mathbf{F}^I, \zeta^S). \quad (5.23)$$

Note that $\partial_k F_{\alpha\beta}^{I-1} = -F_{\alpha\gamma}^{I-1} F_{\delta\beta}^{I-1} \partial_k F_{\gamma\delta}^I$. Global integrability of \mathbf{F}^{E-1} suggests that stress acting on the boundary of each volume element can be relaxed (in conjunction with local rotation field \mathbf{R}^{E-1}) so that \bar{B} is a globally compatible configuration, presuming that the crystal is simply connected in configuration B . Recall that in the theory of continuously distributed dislocations, dislocation core volumes and displacement jumps across internal slipped surfaces are not resolved explicitly, so simple connectivity of a deformed body (B) containing dislocation densities becomes possible (25). Statistically stored dislocations ζ^S exert no long-range residual elastic fields associated with incompatibility, but still contribute to (5.23) through short-range and core energies.

Typical gradient-type crystal plasticity models (2, 15, 35) invoke the usual two-term decomposition $\mathbf{F} = \mathbf{F}^E \mathbf{F}^P$ of (1.1), and the presence of dislocations within a local volume element is indicated by $\nabla \times \mathbf{F}^P \neq 0$ as in (5.20). However, this description alone does not account for statistically stored dislocations, which may exist regardless of whether or not the curl of the plastic deformation gradient vanishes; a non-vanishing curl only indicates the presence of geometrically necessary dislocations. In pure ductile metals under homogeneous deformation, statistically stored dislocations would be expected to contribute most strongly to strain hardening and stored energy. Furthermore, since $\det \mathbf{F}^P = 1$ in slip-based crystal plasticity theory, local residual dilatation cannot be captured by such models invoking (1.1). In contrast, and though perhaps more complicated, the present theory invoking (1.2) can account for residual dilatation (as well as residual lattice shape change) via the \mathbf{F}^I term, which in turn is affected by the total dislocation density, including both geometrically necessary and statistically stored dislocations.

5.3 Constitutive relations and dissipation inequality

Under the present idealisation of isothermal conditions, the local balance of energy and entropy inequality are (35)

$$\dot{U} = \boldsymbol{\tau} : \mathbf{L}, \quad \dot{U} - \dot{\Psi} \geq 0, \quad (5.24)$$

where U is internal energy per unit reference volume, $\boldsymbol{\tau} = J\boldsymbol{\sigma}$ is macroscopic symmetric Kirchhoff stress with $\boldsymbol{\sigma}$ Cauchy stress and $J = \det \mathbf{F} = J^E J^I J^P = J^E J^I$, and Ψ represents free energy density. Using (5.10) and (5.16),

$$\begin{aligned} \dot{U} &= \boldsymbol{\tau} : [\mathbf{L}^E + \mathbf{F}^E \mathbf{F}^I (\mathbf{L}^P + \mathbf{L}^I) \mathbf{F}^{I-1} \mathbf{F}^{E-1}] \\ &= (\mathbf{F}^{E-1} \boldsymbol{\tau} \mathbf{F}^{E-T}) : \dot{\boldsymbol{\epsilon}} + b \sum_k \tau^{(k)} \zeta^{(k)} \nu^{(k)} + \frac{b}{2\sqrt{\pi}} \sum_k \tau^{(k)} \dot{\zeta}^{(k)} (\zeta^{(k)})^{-1/2} \\ &\quad - 3P \sum_k \frac{\partial \varphi}{\partial \zeta^{(k)}} \dot{\zeta}^{(k)} + \boldsymbol{\tau} : \hat{\mathbf{L}}_{\text{core}}^I \end{aligned} \quad (5.25)$$

is total external stress power, and

$$\dot{\Psi} = \frac{\partial \Psi}{\partial \boldsymbol{\epsilon}} : \dot{\boldsymbol{\epsilon}} + \frac{\partial \Psi}{\partial \xi} \dot{\xi}, \quad (5.26)$$

is the free energy rate, where resolved shear stress and reference pressure (energy per unit reference volume) are

$$\tau^{(k)} \stackrel{\text{def}}{=} \boldsymbol{\tau} : (\hat{\mathbf{s}}^{(k)} \otimes \hat{\mathbf{m}}^{(k)}) = \tau_{ij} \hat{s}_i^{(k)} \hat{m}_j^{(k)}, \quad P \stackrel{\text{def}}{=} -\frac{1}{3} \tau_{kk} = Jp. \quad (5.27)$$

Substituting into the second of (5.24) and considering admissible processes,

$$\boldsymbol{\tau}(\mathbf{F}^E, \xi) = \mathbf{F}^E \frac{\partial \Psi}{\partial \boldsymbol{\epsilon}} \mathbf{F}^{E-T}, \quad h(\boldsymbol{\epsilon}, \xi) \stackrel{\text{def}}{=} \frac{\partial \Psi}{\partial \xi}; \quad (5.28)$$

$$b \sum_k \tau^{(k)} \zeta^{(k)} \nu^{(k)} + \frac{b}{2\sqrt{\pi}} \sum_k \tau^{(k)} \{\dot{\zeta}^{(k)} (\zeta^{(k)})^{-1/2}\} - 3P \sum_k \frac{\partial \varphi}{\partial \zeta^{(k)}} \dot{\zeta}^{(k)} + \boldsymbol{\tau} : \hat{\mathbf{L}}_{\text{core}}^I - h \dot{\xi} \geq 0. \quad (5.29)$$

Equations (5.28) are the hyperelastic stress-strain law and definition of the thermodynamic conjugate force to internal state variable ξ . If (5.15) applies, then dissipation inequality (5.29) becomes

$$b \sum_k \tau^{(k)} \zeta^{(k)} \nu^{(k)} + \boldsymbol{\tau} : \hat{\mathbf{L}}_{\text{core}}^I + \sum_k \dot{\zeta}^{(k)} \left[\frac{b}{2\sqrt{\pi}} \tau^{(k)} (\zeta^{(k)})^{-1/2} - 3P \frac{\partial \varphi}{\partial \zeta^{(k)}} - \frac{b}{2} h \zeta^{-1/2} \right] \geq 0. \quad (5.30)$$

Consider each term in (5.30). The first term is dissipation from slip of mobile dislocations. The second is stress power associated with deformation of the volume element from core effects, noting that only the symmetric part of $\hat{\mathbf{L}}_{\text{core}}^I$ contributes. Remaining terms in square brackets are associated directly with dislocation density rates $\dot{\zeta}^{(k)}$. The first term is due to shearing associated with the rate of \mathbf{F}^I , in the simple case of an isolated dislocation resulting from the linear elastic contribution to $\boldsymbol{\beta}_{\text{lin}}^I$. The second is due to dilatation associated with the rate of \mathbf{F}^I , for an isolated dislocation resulting from the non-linear elastic contribution to $\boldsymbol{\beta}_{\text{nonlin}}^I$. The $b^2 h$ term represents free energy storage associated with microscopic strain energy, core energy and interaction energies of dislocations within the volume element. Dissipation from slip is positive when resolved shear stress $\tau^{(k)}$ and dislocation velocity $\nu^{(k)}$ share the same sign. Remaining terms can contribute positively or negatively to dissipation/storage of energy because algebraic signs of $\dot{\zeta}^{(k)}$ and its multipliers are unrestricted; dislocation rates may be positive or negative as defects enter or exit the volume, or are generated or annihilated.

6. Examples

6.1 Simple shear

Consider a single crystalline cylindrical volume element of initial volume $V = \pi R^2 L$ with L parallel to unit vector \mathbf{e}_3 . Let this element be subject to homogeneous simple shear deformation of the form

$$\mathbf{F} = \mathbf{F}^E \mathbf{F}^I \mathbf{F}^P = \mathbf{1} + \Xi \mathbf{e}_1 \otimes \mathbf{e}_2 = \mathbf{1} + \Xi \mathbf{s} \otimes \mathbf{m}. \quad (6.1)$$

Applied shear deformation is Ξ , and the crystal is assumed perfectly oriented for single slip, with $\mathbf{s} = \mathbf{e}_1$ and $\mathbf{m} = \mathbf{e}_2$. For this 2D problem, dislocation density ζ consists of a single family of edge dislocations with $\mathbf{b} = b\mathbf{s}$. Since $\mathbf{s} \cdot \mathbf{m} = 0$, cumulative plastic deformation is of the form in (3.13):

$$\mathbf{F}^P = \exp(\gamma \mathbf{s} \otimes \mathbf{m}) = \mathbf{1} + \gamma \mathbf{s} \otimes \mathbf{m}, \quad (6.2)$$

with cumulative slip γ to be determined in the analysis as a function of Ξ . A rate independent yield criterion is used here since Ξ is increased monotonically at a fixed rate:

$$\tau \stackrel{\text{def}}{=} \boldsymbol{\tau} : (\hat{\mathbf{s}} \otimes \hat{\mathbf{m}}) \leq \tau_0 + \alpha G b \sqrt{\zeta}, \quad (6.3)$$

with τ the resolved Kirchhoff stress, τ_0 the initial yield strength, and α a constant in the usual Taylor hardening model (36). Linear hardening with modulus H is assumed such that $H\gamma = \alpha b \sqrt{\zeta}$, leading to the following dimensionless yield criterion and evolution equation for dislocation density:

$$\tau/G \leq \tau_0/G + H\gamma; \quad \zeta = [H\gamma/(\alpha b)]^2. \quad (6.4)$$

Residual lattice deformation is, from (3.30), the second of (6.4), and assuming null core traction,

$$\mathbf{F}^I(\gamma) = \mathbf{1} + \frac{H\gamma}{\sqrt{\pi\alpha}} \mathbf{s} \otimes \mathbf{m} - \frac{A H^2 \gamma^2}{4 \alpha^2} \ln \frac{\pi H^2 \gamma^2}{\alpha^2} (\mathbf{s} \otimes \mathbf{s} + \mathbf{m} \otimes \mathbf{m}). \quad (6.5)$$

Under isothermal conditions, and omitting coupling between internal state variable $\xi = b\sqrt{\zeta}$ and elastic Green strain $\boldsymbol{\epsilon} = \frac{1}{2}(\mathbf{F}^{E\text{T}} \mathbf{F}^E - \mathbf{1})$, (5.16) and (5.17) can be combined to give free energy density Ψ of the form below, to order three in elastic strain:

$$\Psi = \frac{1}{2} C_{\alpha\beta\gamma\delta} \epsilon_{\alpha\beta} \epsilon_{\gamma\delta} + \frac{1}{6} C_{\alpha\beta\gamma\delta\epsilon\phi} \epsilon_{\alpha\beta} \epsilon_{\gamma\delta} \epsilon_{\epsilon\phi} + \iota(\xi), \quad (6.6)$$

where second- and third-order elastic constants $C_{\alpha\beta\gamma\delta}$ and $C_{\alpha\beta\gamma\delta\epsilon\phi}$ are described in Appendix A, and stored energy of cold work ι is inconsequential in the stress-strain response in this example. Kirchhoff stress is, from (5.28),

$$\boldsymbol{\tau}(\mathbf{F}^E) = \mathbf{F}^E \frac{\partial \Psi}{\partial \boldsymbol{\epsilon}} \mathbf{F}^{E\text{T}} = \mathbf{J} \boldsymbol{\sigma}, \quad (6.7)$$

with $\boldsymbol{\sigma}$ the Cauchy stress, noting $J = \det \mathbf{F} = J^E J^I = 1$ from (6.1) and (6.2).

Solution of the problem proceeds as follows. Deformation Ξ is updated incrementally. For each increment, use of (6.1), (6.2), (6.5), and (6.7) enables iterative solution of yield condition (6.4)

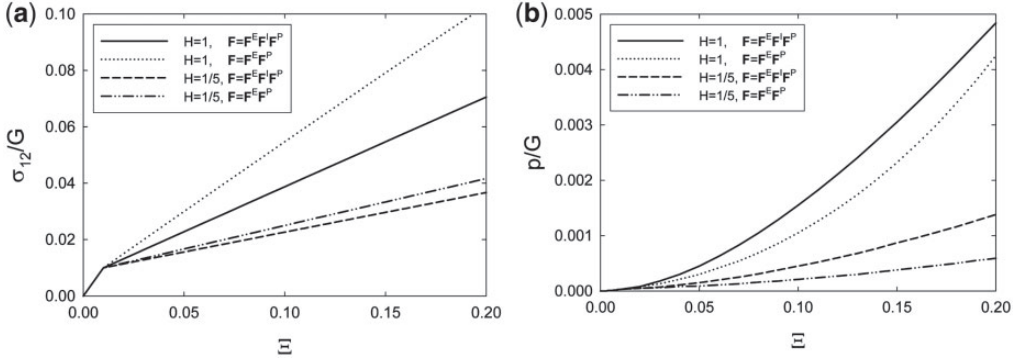


Fig. 5 Shear stress (a) and Cauchy pressure (b) predicted using three-term ($\mathbf{F} = \mathbf{F}^E \mathbf{F}^I \mathbf{F}^P$) and two-term ($\mathbf{F} = \mathbf{F}^E \mathbf{F}^P$) models for single crystal in simple shear and oriented for single slip, with hardening modulus H

for slip γ , with inequality holding during elastic loading ($\gamma = 0$) and equality holding upon yield ($\gamma > 0$). With $\mathbf{F}(\Xi)$ and γ known, all other quantities of interest ($\boldsymbol{\sigma}$, ζ , etc.) can be computed. Representative material properties are taken from Table A.1 of Appendix A, leading to $A = \frac{1}{12}$ as in Section 3. Also, $\tau_0 = \frac{1}{100}G$, $\alpha = \frac{1}{2}$, and two values of H ($\frac{1}{5}$ and 1) are considered.

Shear stress σ_{12} and pressure $p = -\frac{1}{3}\text{tr}\boldsymbol{\sigma}$ are shown in Figs 5(a) and 5(b). Results labelled ‘ $\mathbf{F} = \mathbf{F}^E \mathbf{F}^P$ ’, are obtained by setting $\mathbf{F}^I = \mathbf{1}$ instead of (6.5), with all other model features the same as for the three-term theory with $\mathbf{F} = \mathbf{F}^E \mathbf{F}^I \mathbf{F}^P$ described above. Shear stress increases in the plastic regime with increasing linear hardening modulus H , as expected. Shear stresses are lower when the three-term model is used because \mathbf{F}^I accommodates some of the applied shear strain that would otherwise be accommodated by \mathbf{F}^E . Pressures are higher when the three-term model is used because \mathbf{F}^I includes dilatation $J^I = 1/J^E > 1$. Although nearly the same shear stress response could be obtained by selecting different values of H for two- and three-term models, only the three-term theory is able to properly account for pressure rise resulting from dilatation due to dislocations; such dilatation has been observed in experiments (26) and atomic simulations (21, 28).

6.2 Uniaxial compression

Now consider a single crystalline cylindrical volume element of initial volume $V = \pi R^2 L$ with L parallel to unit vector \mathbf{e}_1 . Let this element be subject to homogeneous uniaxial strain of the form

$$\mathbf{F} = \mathbf{F}^E \mathbf{F}^I \mathbf{F}^P = (1 - \Xi)\mathbf{e}_1 \otimes \mathbf{e}_1 + \mathbf{e}_2 \otimes \mathbf{e}_2 + \mathbf{e}_3 \otimes \mathbf{e}_3. \quad (6.8)$$

Applied compression is $\Xi \geq 0$, and the crystal structure is taken as FCC, with cube axes [100], [010] and [001] parallel to \mathbf{e}_1 , \mathbf{e}_2 and \mathbf{e}_3 , so compression occurs along [100] in this problem. This example is representative of planar shock compression of a cubic single crystal (37), though here temperature/entropy effects are omitted for simplicity. From symmetry (37), 8 of 12 possible $\{111\}\langle 110 \rangle$ slip systems are active upon yielding ($k = 1, 2, \dots, 8$), each with the same cumulative slip $\gamma = \gamma^{(k)} = \int \dot{\gamma}^{(k)} dt$. For monotonic loading, integration of (5.3) results in plastic deformation

of the following form, to order three in γ :

$$\begin{aligned} \mathbf{F}^{\text{P}} &= \exp\left(\gamma \sum_k \mathbf{s}^{(k)} \otimes \mathbf{m}^{(k)}\right) \\ &\approx \mathbf{1} + \gamma \sum_k \mathbf{s}^{(k)} \otimes \mathbf{m}^{(k)} + \frac{\gamma^2}{2} \left(\sum_k \mathbf{s}^{(k)} \otimes \mathbf{m}^{(k)}\right)^2 + \frac{\gamma^3}{6} \left(\sum_k \mathbf{s}^{(k)} \otimes \mathbf{m}^{(k)}\right)^3, \end{aligned} \quad (6.9)$$

with cumulative slip γ to be determined in the analysis as a function of Ξ . Equations similar to (6.3) and (6.4) apply:

$$\boldsymbol{\tau}^{(k)} = \boldsymbol{\tau} : (\hat{\mathbf{s}}^{(k)} \otimes \hat{\mathbf{m}}^{(k)}) \leq \tau_0 + \alpha G b \sqrt{\zeta} = \tau_0 + G H \gamma; \quad \zeta = [H \gamma / (\alpha b)]^2. \quad (6.10)$$

Here $\zeta = \sum_k \zeta^{(k)} = 8 \zeta^{(k)}$ again is assumed to consist entirely of straight edge dislocations with $\mathbf{b}^{(k)} = b \mathbf{s}^{(k)}$. The linear elastic contribution to \mathbf{F}^{I} is given by analogue of (3.18) and (5.4); the non-linear elastic contribution a volume change of the form in (3.22), (3.23), (5.6), and (5.8); core traction is again omitted for simplicity. These assertions, with the second of (6.10), result in

$$\mathbf{F}^{\text{I}}(\gamma) = \mathbf{1} + \frac{H \gamma}{\sqrt{8 \pi \alpha}} \sum_k \mathbf{s}^{(k)} \otimes \mathbf{m}^{(k)} - \frac{A}{6} \frac{H^2 \gamma^2}{\alpha^2} \ln \frac{\pi H^2 \gamma^2}{\alpha^2} \mathbf{e}_\alpha \otimes \mathbf{e}_\alpha. \quad (6.11)$$

The non-linear hyperelastic response is again dictated by (6.6) and (6.7). The same numerical solution procedure and material properties used in Section 6.1 apply here.

Axial true stress $-\sigma_{11}$ and dislocation density ζ are shown in Figs 6(a) and 6(b), the latter normalised by $\zeta_{\text{max}} = \frac{1}{\pi b^2}$. Results labelled ' $\mathbf{F} = \mathbf{F}^{\text{E}} \mathbf{F}^{\text{P}}$ ', are obtained by setting $\mathbf{F}^{\text{I}} = \mathbf{1}$ instead of (6.11), with all other model features the same as for the three-term theory with $\mathbf{F} = \mathbf{F}^{\text{E}} \mathbf{F}^{\text{I}} \mathbf{F}^{\text{P}}$. Axial stresses [Fig. 6(a)] are identical for all cases until yield is attained at $\Xi = 1 - J \approx 0.017$, which would correspond to the Hugoniot elastic limit in a planar shock experiment. Stresses increase in the plastic regime with increasing linear hardening modulus H , as expected. Differences between

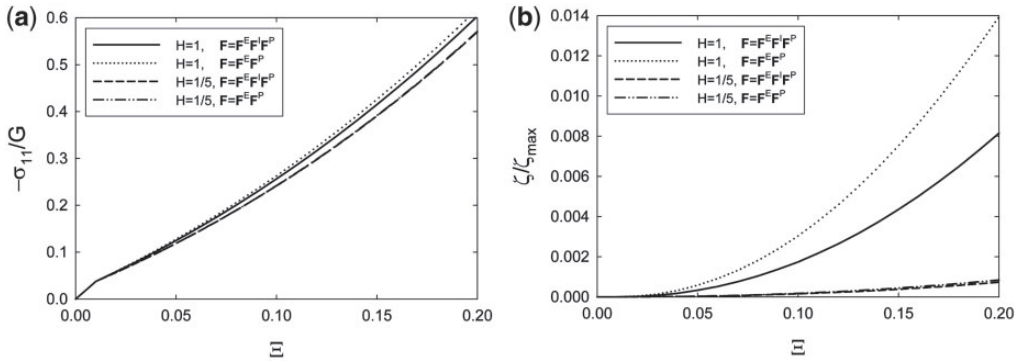


Fig. 6 Axial stress (a) and dislocation density (b) predicted using three-term ($\mathbf{F} = \mathbf{F}^{\text{E}} \mathbf{F}^{\text{I}} \mathbf{F}^{\text{P}}$) and two-term ($\mathbf{F} = \mathbf{F}^{\text{E}} \mathbf{F}^{\text{P}}$) models for FCC single crystal compressed along $[100]$, with hardening modulus H

two- and three-term models are negligible for the lower hardening modulus $H = \frac{1}{5}$, but not for higher hardening with $H = 1$. Dislocation densities [Fig. 6(b)] predicted by the two-term theory increasingly exceed those predicted by the three-term theory as γ or H is increased. At $\Xi \approx 0.2$, dislocation densities predicted using $H = \frac{1}{5}$ are of comparable magnitude to maximum densities observed during shock compression experiments on Cu and Cu-Al alloys (38).

6.3 Discussion

The presentation in Sections 6.1 and 6.2 demonstrates how a constitutive model incorporating the three-term decomposition (1.2) can be implemented, in a straightforward way, for crystal volumes undergoing homogeneous deformation. Results have indicated, for representative material properties, the applied strain required for the \mathbf{F}^I term to significantly affect stresses. Differences between the present theory and the usual two-term description become most apparent at large strain in crystals with strong hardening associated with defect accumulation. Validity of the theory for addressing residual lattice deformation has been established, within an order of magnitude, by comparison with results of atomic simulation in Table 1. Comparison of theoretically predicted dilatation with experiments reporting energy of cold work and residual volume change has been presented elsewhere (17, 26), wherein again order-of-magnitude accuracy has been confirmed. As suggested by derivations and calculations in Sections 3 and 4 for edge and screw dislocations, the magnitude of residual lattice contribution from defect(s) within a local volume, \mathbf{F}^I , can exceed several percent as the theoretical maximum dislocation density is approached, but is small for dilute dislocation concentrations. Here ‘magnitude of’ refers to the largest absolute value of any stretch component. Bulk dislocation densities of up to 2–10 per cent of the theoretical maximum have been observed in atomic and discrete dynamic simulations of shock loading (39), which would impart substantial contributions to \mathbf{F}^I with a corresponding effect on observed pressure-density behaviour in shock compression experiments (30). Even if the bulk dislocation density is small when averaged over a large volume of crystal, the local dislocation density at volume elements comprising dislocation cells and cell walls during latter stages of work hardening may be quite large (for example, approaching the theoretical maximum), so the magnitude of \mathbf{F}^I would be substantial for those elements.

More extensive algorithms and numerical simulations are needed for applying the theory to problems involving heterogeneous deformation; such developments are reserved for future work. For example, local regions with dislocation densities on the order of 10^{16} m^{-2} have been reported for a nickel crystal subjected to wedge indentation (40), corresponding to $\zeta/\zeta_{\max} \approx 2 \times 10^{-3}$. Referring to results in Table 1, \mathbf{F}^I would be expected to be non-trivial in such regions.

By definition, $\mathbf{F}^I \rightarrow \mathbf{1}$ as the dislocation content in a volume element goes to zero ($\zeta \rightarrow 0$). If, as in the model of Sections 6.1 and 6.2, plastic strain hardening results from accumulated dislocations, then $\mathbf{F}^I \rightarrow \mathbf{1}$ for an elastic-perfectly plastic crystal through which dislocations pass but do not accumulate.

Several (co)authored previous works (7, 8, 9, 17) proposed three-term decompositions but did not derive their origins in the context of elastic solutions for single dislocations and did not develop constitutive frameworks identical to that in Section 5. Content in the monograph (12) mostly summarises content of such prior work, in Section 9.1.3 leaving the physical definition of the third term ambiguous in general thermomechanical analysis, similar to (5). A different three-term decomposition of the deformation gradient, written $\mathbf{F}^S = \mathbf{F}^{LC}\mathbf{F}^{LD}\mathbf{F}^D$, has also recently been developed (14). In this different approach, following early concepts of dislocation field theory (1, 4), $\mathbf{F}^S = \mathbf{F}$ is the total shape deformation of a material element, \mathbf{F}^D represents rigid slip due

to dislocations currently within the element *and* those that have passed completely through, F^{LD} is lattice deformation that returns the element to a compact state (residual elastic and core effects), and F^{LC} is recoverable lattice deformation associated with loading of the external boundary of the entire body. Generally, F^D and F^{LD} are incompatible fields (they do not obey integrability conditions), but F^{LC-1} is compatible and is the spatial gradient of a vector field. Both the present approach and that in (14) derive a multiplicative decomposition for single edge and screw dislocations, and then generalise to multiple defects. However, steps followed in each approach differ, leading to different interpretations of the third (middle) term in the decomposition associated with residual lattice distortion. This leads to different numerical results in the present work and in (14). Example calculations for simple shear and uniaxial compression in Sections 6.1 and 6.2 are the first such reported using the current three-term description and have not been presented elsewhere. Appendices herein contain non-linear elastic derivations and treatment of anisotropy not given in (14).

7. Conclusions

A three-term multiplicative decomposition for an element of single crystal containing dislocations has been derived. In addition to usual terms associated with elastic deformation and cumulative dislocation slip through the element, a third term has been incorporated that accounts for defects within. This third term is further divided into contributions from the incompletely slipped surface (a ‘linear’ term), elasticity, and core effects. Expressions have been derived, and magnitudes estimated, for contributions to this third term for cylindrical elements containing a single edge or screw dislocation line. For dislocation densities approaching the theoretical limit, such magnitudes may be comparable to applied elastic strains needed to initiate slip. Upon generalisation of the theory to crystals with multiple defects, appropriate general forms of free energy functions have been suggested and analysed in the context of the three-term decomposition. The theory has been implemented in constitutive model calculations for simple shear and uniaxial strain compression, with differences in results from those of usual two-term crystal plasticity apparent for large strains and strong plastic hardening. Primary advantages of the proposed three-term description are (i) its precise delineation of contributions from dislocation motion and dislocation generation to irreversible deformation, and (ii) its ability to quantify local residual elastic strains, including volume changes. Neither phenomenon can be captured by two-term crystal plasticity wherein the rate of plastic deformation results only from slip rates described by the usual Orowan equation.

References

1. B. A. Bilby, L. R. T. Gardner and A. N. Stroh, Continuous distributions of dislocations and the theory of plasticity, *Proc. 9th Int. Congress of Applied Mechanics*, vol. 8 (University de Bruxelles, Brussels 1957) 35–44.
2. E. Kröner, Allgemeine kontinuumstheorie der versetzungen und eigenspannungen, *Arch. Rat. Mech. Anal.* **4** (1960) 273–334.
3. N. Fox, On the continuum theories of dislocations and plasticity, *Quart. J. Mech. Appl. Math.* **21** (1968) 67–75.
4. B. A. Bilby, L. R. T. Gardner, A. Grinberg and M. Zorawski, Continuous distributions of dislocations VI. Non-metric connexions, *Proc. R. Soc. Lond. A* **292** (1966) 105–121.
5. J. Kratochvíl, Finite-strain theory of inelastic behavior of crystalline solids, *Foundations of Plasticity* (ed. A. Sawczuk; Noordhoff, Leyden 1972) 401–415.

6. A. Lion, Constitutive modelling in finite thermoviscoplasticity: a physical approach based on nonlinear rheological models, *Int. J. Plast.* **16** (2000) 469–494.
7. J. D. Clayton and D. L. McDowell, A multiscale multiplicative decomposition for elastoplasticity of polycrystals, *Int. J. Plast.* **19** (2003) 1401–1444.
8. J. D. Clayton, D. L. McDowell and D. J. Bammann, A multiscale gradient theory for single crystalline elastoviscoplasticity, *Int. J. Eng. Sci.* **42** (2004) 427–457.
9. J. D. Clayton, D. J. Bammann and D. L. McDowell, A geometric framework for the kinematics of crystals with defects, *Phil. Mag.* **85** (2005) 3983–4010.
10. J. M. Gerken and P. R. Dawson, A crystal plasticity model that incorporates stresses and strains due to slip gradients, *J. Mech. Phys. Solids* **56** (2008) 1651–1672.
11. D. L. Henann and L. Anand, A large deformation theory for rate-dependent elastic-plastic materials with combined isotropic and kinematic hardening, *Int. J. Plast.* **25** (2009) 1833–1878.
12. J. D. Clayton, *Nonlinear Mechanics of Crystals* (Springer, Dordrecht 2011).
13. K. I. Elkhodary and M. A. Zikry, A fracture criterion for finitely deforming crystalline solids—the dynamic fracture of single crystals, *J. Mech. Phys. Solids* **59** (2011) 2007–2022.
14. J. D. Clayton, C. S. Hartley and D. L. McDowell, The missing term in the decomposition of finite deformation, *Int. J. Plast.* **52** (2014) 51–76.
15. C. Teodosiu. *Elastic Models of Crystal Defects* (Springer, Berlin 1982).
16. R. A. Toupin and R. S. Rivlin. Dimensional changes in crystals caused by dislocations, *J. Math. Phys.* **1** (1960) 8–15.
17. J. D. Clayton and D. J. Bammann. Finite deformations and internal forces in elastic-plastic crystals: interpretations from nonlinear elasticity and anharmonic lattice statics, *J. Eng. Mater. Tech.* **131** (2009) 041201.
18. L. M. Zubov and E. S. Nikitin, An exact solution to the problem of edge dislocation in a nonlinear elastic medium, *Sov. Phys. Doklady* **39** (1994) 38–41.
19. A. Seeger, C. Teodosiu and P. Petrasch, Second-order effects in the anisotropic elastic field of a straight edge dislocation, *Phys. Stat. Solidi B* **67** (1975) 207–224.
20. J. Li, C. Z. Wang, J. P. Chang, W. Cai, V. V. Bulatov, K. M. Ho and S. Yip, Core energy and Peierls stress of a screw dislocation in bcc molybdenum: a periodic tight-binding study, *Phys. Rev. B* **70** (2004) 104–113.
21. J. E. Sinclair, P. C. Gehlen, R. G. Hoagland and J. P. Hirth, Flexible boundary conditions and nonlinear geometric effects in atomic dislocation modeling, *J. Appl. Phys.* **49** (1978) 3890–3897.
22. P. C. Gehlen, J. P. Hirth, R. C. Hoagland and M. F. Kanninen, A new representation of the strain field associated with the cube-edge dislocation in a model of α -iron, *J. Appl. Phys.* **43** (1972) 3921–3933.
23. P. S. White, Elastic-plastic solids as simple materials, *Quart. J. Mech. Appl. Math.* **28** (1975) 483–496.
24. L. M. Zubov, *Nonlinear Theory of Dislocations and Disclinations in Elastic Bodies* (Springer, Berlin 1997).
25. J. R. Willis, Second-order effects of dislocations in anisotropic crystals, *Int. J. Eng. Sci.* **5** (1967) 171–190.
26. T. W. Wright, Stored energy and plastic volume change, *Mech. Mater.* **1** (1982) 185–187.
27. E. B. Webb, J. A. Zimmerman and S. C. Seel, Reconsideration of continuum thermomechanical quantities in atomic scale simulations, *Math. Mech. Solids* **13** (2008) 221–266.

28. E. Clouet, L. Ventelon and F. Willaime, Dislocation core field II. Screw dislocation in iron. *Phys. Rev. B* **84** (2011) 224107.
29. R. W. Armstrong and F. J. Zerilli, High rate straining of tantalum and copper, *J. Phys. D* **43** (2010) 492002.
30. J. D. Clayton, A continuum description of nonlinear elasticity, slip and twinning, with application to sapphire, *Proc. R. Soc. Lond. A* **465** (2009) 307–334.
31. J. R. Willis, The elastic interaction energy of dislocation loops in anisotropic media, *Quart. J. Mech. Appl. Math.* **18** (1965) 419–433.
32. J. D. Clayton and P. W. Chung, An atomistic-to-continuum framework for nonlinear crystal mechanics based on asymptotic homogenization, *J. Mech. Phys. Solids* **54** (2006) 1604–1639.
33. J. D. Clayton, D. J. Bammann and D. L. McDowell, Anholonomic configuration spaces and metric tensors in finite elastoplasticity, *Int. J. Non-Linear Mech.* **39** (2004) 1039–1049.
34. J. D. Clayton, On anholonomic deformation, geometry, and differentiation, *Math. Mech. Solids* **17** (2012) 702–735.
35. M. E. Gurtin, A finite-deformation, gradient theory of single-crystal plasticity with free energy dependent on the accumulation of geometrically necessary dislocations, *Int. J. Plast.* **26** (2010) 1073–1096.
36. G. E. Beltz, J. R. Rice, C. F. Shih and L. Xia, A self-consistent model for cleavage in the presence of plastic flow, *Acta Mater.* **44** (1996) 3943–3954.
37. J. N. Johnson, O. E. Jones and T. E. Michaels, Dislocation dynamics and single-crystal constitutive relations: shock-wave propagation and precursor decay, *J. Appl. Phys.* **41** (1970) 2330–2339.
38. A. Rohatgi and K. S. Vecchio, The variation of dislocation density as a function of the stacking fault energy in shock-deformed FCC materials, *Mater. Sci. Eng. A* **328** (2002) 256–266.
39. M. A. Shehadeh, E. M. Bringa, H. M. Zbib, J. M. McNaney and B. A. Remington, Simulation of shock-induced plasticity including homogeneous and heterogeneous dislocation nucleations, *Appl. Phys. Lett.* **89** (2006) 171918.
40. J. W. Kysar, Y. Saito, M. S. Oztop, D. Lee and W. T. Huh, Experimental lower bounds on geometrically necessary dislocation density, *Int. J. Plast.* **26** (2010) 1097–1123.
41. M. W. Guinan and D. J. Steinberg, Pressure and temperature derivatives of the isotropic polycrystalline shear modulus for 65 elements, *J. Phys. Chem. Solids* **35** (1974) 1501–1512.
42. D. J. Steinberg, Some observations regarding the pressure dependence of the bulk modulus, *J. Phys. Chem. Solids* **43** (1982) 1173–1175.
43. A. J. E. Foreman, Dislocation energies in anisotropic crystals, *Acta Metall.* **3** (1955) 322–330.
44. J. D. Clayton, Dynamic plasticity and fracture in high density polycrystals: constitutive modeling and numerical simulation, *J. Mech. Phys. Solids* **53** (2005) 261–301.
45. J. J. Gilman, *Electronic Basis of the Strength of Materials* (Cambridge University Press, Cambridge 2003).

APPENDIX A

Non-linear elastic coefficients

Let $u_\alpha(X_\beta)$ denote elastic displacement and X_β Lagrangian coordinates; Green elastic strain is

$$E_{\alpha\beta} = \frac{1}{2} \left(\frac{\partial u_\alpha}{\partial X_\beta} + \frac{\partial u_\beta}{\partial X_\alpha} + \frac{\partial u_\gamma}{\partial X_\alpha} \frac{\partial u_\gamma}{\partial X_\beta} \right). \quad (\text{A.1})$$

Strain energy density W written as a Taylor polynomial is

$$W = \frac{1}{2}C_{\alpha\beta\gamma\delta}E_{\alpha\beta}E_{\gamma\delta} + \frac{1}{6}C_{\alpha\beta\gamma\delta\epsilon\phi}E_{\alpha\beta}E_{\gamma\delta}E_{\epsilon\phi} + \dots \quad (\text{A.2})$$

For homogeneous isotropic materials, elastic constant tensors are of the form

$$C_{\alpha\beta\gamma\delta} = \lambda(\delta_{\alpha\beta}\delta_{\gamma\delta}) + G(\delta_{\alpha\gamma}\delta_{\beta\delta} + \delta_{\alpha\delta}\delta_{\beta\gamma}), \quad (\text{A.3})$$

$$\begin{aligned} C_{\alpha\beta\gamma\delta\epsilon\phi} = & \nu_1[\delta_{\alpha\beta}\delta_{\gamma\delta}\delta_{\epsilon\phi}] \\ & + \nu_2[\delta_{\alpha\beta}(\delta_{\gamma\epsilon}\delta_{\delta\phi} + \delta_{\gamma\phi}\delta_{\delta\epsilon}) + \delta_{\gamma\delta}(\delta_{\alpha\epsilon}\delta_{\beta\phi} + \delta_{\alpha\phi}\delta_{\beta\epsilon}) + \delta_{\epsilon\phi}(\delta_{\alpha\gamma}\delta_{\beta\delta} + \delta_{\alpha\delta}\delta_{\beta\gamma})] \\ & + \nu_3[\delta_{\alpha\gamma}(\delta_{\beta\epsilon}\delta_{\delta\phi} + \delta_{\beta\phi}\delta_{\delta\epsilon}) + \delta_{\beta\delta}(\delta_{\alpha\epsilon}\delta_{\gamma\phi} + \delta_{\alpha\phi}\delta_{\gamma\epsilon}) \\ & + \delta_{\alpha\delta}(\delta_{\beta\epsilon}\delta_{\gamma\phi} + \delta_{\beta\phi}\delta_{\gamma\epsilon}) + \delta_{\beta\gamma}(\delta_{\alpha\epsilon}\delta_{\delta\phi} + \delta_{\alpha\phi}\delta_{\delta\epsilon})]. \end{aligned} \quad (\text{A.4})$$

Let C_{IJ} and C_{IJK} denote second- and third-order constants in Voigt notation, where indices 1, 2, . . . 6. Second-order elastic constants obey the familiar relations

$$\lambda = C_{12}, \quad G = C_{44} = \frac{1}{2}(C_{11} - C_{12}), \quad K = \lambda + \frac{2}{3}G, \quad \nu = \frac{\lambda}{2(\lambda + G)}, \quad (\text{A.5})$$

where G , K and ν are shear modulus, bulk modulus and Poisson's ratio in the reference state. Third-order elastic constants obey

$$\nu_1 = C_{123}, \quad \nu_2 = C_{144} = \frac{1}{2}(C_{112} - C_{123}), \quad \nu_3 = C_{456} = \frac{1}{8}(C_{111} - 3C_{112} + 2C_{123}). \quad (\text{A.6})$$

Let $\hat{K}(p)$ and $\hat{G}(p)$ denote incremental bulk and shear moduli of an isotropic elastic solid subjected to dilatation induced by Cauchy pressure p . Then **(15, 41)**

$$K' \stackrel{\text{def}}{=} (d\hat{K}/dp)|_{p=0} = -[\nu_1 + 2\nu_2 + (8/9)\nu_3]/K, \quad (\text{A.7})$$

$$G' \stackrel{\text{def}}{=} (d\hat{G}/dp)|_{p=0} = -[\lambda + G + \nu_2 + (4/3)\nu_3]/K. \quad (\text{A.8})$$

Ultrasonic measurements and various high pressure experiments suggest that the pressure derivative of the bulk modulus in the reference state obeys $2 < K' < 7$ for most pure elemental crystalline solids, with $3 < K' < 6$ typical **(42)**. Experimental data also suggest that the pressure derivative of the thermodynamic shear modulus in the reference state obeys $0 < G' < 3$ for most pure elements **(41)**. Representative values used in this article are tabulated in Table A.1. Note $\lambda = G \Leftrightarrow \nu = \frac{1}{4}$, whereas for crystalline metals and minerals typically $0.05 < \nu < 0.45$.

Table A.1 Representative elastic constants and Burgers magnitude b .

λ/G	K'	G'	ν_2/G	ν_3/G	b [m]
1	4	1	$-\frac{11}{7}$	$-\frac{11}{7}$	3×10^{-10}

APPENDIX B

Radial displacement for screw dislocation in non-linear isotropic cylinder

Expressions for c_1 , c_2 and c_3 of (4.12) are listed or newly derived here. Considered only is the case when pressure \hat{p} vanishes on the dislocation core boundary at $\rho = r$. Constant c_3 is (15)

$$c_3 = \frac{b^2(G + \nu_3)}{8\pi^2(\lambda + 2G)}, \quad (\text{B.1})$$

with λ the Lamé modulus and ν_3 a third-order elastic constant. Constants c_1 and c_2 are determined from vanishing traction conditions at $\rho = r$ and $\rho = R$, requiring simultaneous solution of

$$-\frac{2G}{r^2}c_1 + 2(\lambda + G)c_2 + \frac{b^2(G + \nu_3)}{8\pi^2r^2} - Gc_3\frac{\ln r}{r^2} + \frac{b^2(\lambda + \nu_2)}{8\pi^2r^2} = 0, \quad (\text{B.2})$$

$$-\frac{2G}{R^2}c_1 + 2(\lambda + G)c_2 + \frac{b^2(G + \nu_3)}{8\pi^2R^2} - Gc_3\frac{\ln R}{R^2} + \frac{b^2(\lambda + \nu_2)}{8\pi^2R^2} = 0, \quad (\text{B.3})$$

where ν_2 is another third-order elastic constant. After some algebra,

$$c_1 = \frac{b^2}{16\pi^2} \left[1 + \frac{\lambda + \nu_2 + \nu_3}{G} - \frac{(G + \nu_3)(1 - r^2/R^2)\ln r - (r^2/R^2)\ln(R/r)}{(\lambda + 2G)(1 - r^2/R^2)} \right], \quad (\text{B.4})$$

$$c_2 = \frac{b^2}{16\pi^2r^2} \left[\frac{G(G + \nu_3)}{(\lambda + G)(\lambda + 2G)} \right] \left[\frac{\ln r - (r^2/R^2)\ln(R/r)}{1 - r^2/R^2} \right]. \quad (\text{B.5})$$

While generic forms of (B.2) and (B.3) are listed by Teodosiu (15), particular solution (B.4) and (B.5) is newly derived in the present work. Choosing typical values from Table A.1,

$$c_1 \approx \frac{b^2}{80\pi^2} \left[\frac{(r^2/R^2)\ln(R/r) - (1 - r^2/R^2)\ln r}{1 - r^2/R^2} - 5 \right], \quad (\text{B.6})$$

$$c_2 \approx -\frac{b^2}{160\pi^2r^2} \left[\frac{(r^2/R^2)\ln(R/r)}{1 - r^2/R^2} \right], \quad c_3 \approx -\frac{b^2}{40\pi^2}. \quad (\text{B.7})$$

Radial displacement (4.12) at $\rho = R$ becomes

$$\eta(R) = \frac{c_1}{R} + c_2R + c_3\frac{\ln R}{R}, \quad (\text{B.8})$$

where results in Fig. 3 and Table 2 of Section 4 correspond to $r = b$ of Table A.1.

APPENDIX C

Elastic anisotropy

Closed-form analytical elastic solutions for dislocations in anisotropic non-linear elastic solids do not appear to exist, though numerical integration of lengthy and complex approximations available in the literature (19) may

be possible. Analytical solutions can be obtained, however, for volume change $\Delta V/V$ resulting from (3.21) in crystals with cubic symmetry, effectively replacing the first equality in (3.22) or (4.10). In what follows, effects of anisotropy on dilatation are quantified for several kinds of straight dislocations; presumably, effects of anisotropy on deviatoric parts of β_{nonlin}^I are of comparable magnitude, though this cannot be proven at present.

For a density $\zeta = L/V$ of edge, screw, or mixed dislocations, the residual volume change in a cubic crystal can be written as (16, 17)

$$\frac{\Delta V}{V} = \left[\frac{1}{K}(K' - 1)\bar{e} + \frac{1}{G} \left(G' - \frac{G}{K} \right) e' + \frac{1}{Z} \left(Z' - \frac{Z}{K} \right) \tilde{e} \right] \zeta, \quad (\text{C.1})$$

where any three independent second-order elastic constants at the reference state are related by

$$K = \frac{1}{3}(C_{11} + 2C_{12}), \quad G = \frac{1}{2}(C_{11} - C_{12}), \quad Z = C_{44} - G, \quad z = \frac{C_{44}}{G}, \quad (\text{C.2})$$

and Z' is the pressure derivative of tangent stiffness corresponding to Z at the reference state. Dilatational energy per unit dislocation length \bar{e} and deviatoric energies e' and \tilde{e} are (16), (17)

$$\bar{e} = \frac{K}{2L} \int_V \left(\frac{\partial u_\alpha}{\partial X_\alpha} \right)^2 dV, \quad e' = \frac{G}{L} \int_V \left[\frac{1}{2} \left(\frac{\partial u_\alpha}{\partial X_\beta} \frac{\partial u_\beta}{\partial X_\alpha} + \frac{\partial u_\alpha}{\partial X_\alpha} \frac{\partial u_\beta}{\partial X_\beta} \right) - \frac{1}{3} \left(\frac{\partial u_\alpha}{\partial X_\alpha} \right)^2 \right] dV, \quad (\text{C.3})$$

$$\tilde{e} = \frac{Z}{L} \int_V \left[\frac{1}{2} \left(\frac{\partial u_\alpha}{\partial X_\beta} \frac{\partial u_\beta}{\partial X_\alpha} + \frac{\partial u_\alpha}{\partial X_\alpha} \frac{\partial u_\beta}{\partial X_\beta} \right) - \left(\frac{\partial u_1}{\partial X_1} \right)^2 - \left(\frac{\partial u_2}{\partial X_2} \right)^2 - \left(\frac{\partial u_3}{\partial X_3} \right)^2 \right] dV. \quad (\text{C.4})$$

Total dislocation energy per unit length e can be written (43)

$$e = \bar{e} + e' + \tilde{e} = \kappa \frac{b^2}{4\pi} \ln \frac{R}{r}, \quad (\text{C.5})$$

where κ is the energy factor that depends on elastic constants and dislocation geometry. Define

$$\bar{f} \stackrel{\text{def}}{=} \bar{e}/e, \quad f' \stackrel{\text{def}}{=} e'/e, \quad \tilde{f} \stackrel{\text{def}}{=} \tilde{e}/e; \quad \bar{f} + f' + \tilde{f} = 1. \quad (\text{C.6})$$

Furthermore, let κ_{iso} , \bar{f}_{iso} and f'_{iso} denote corresponding quantities in an isotropic elastic solid containing a dislocation having the same geometry and elastic properties (G, K, G', K'), noting that ($Z, Z', \tilde{e}, \tilde{f}$) all vanish for the isotropic case. Then the ratio of residual elastic volume change in a cubic crystal to that in such an isotropic solid can be written

$$\frac{\Delta V}{\Delta V_{\text{iso}}} = \frac{\bar{f}(K' - 1)/K + f'(G' - G/K)/G + \tilde{f}(Z' - Z/K)/Z}{\bar{f}_{\text{iso}}(K' - 1)/K + f'_{\text{iso}}(G' - G/K)/G} \frac{\kappa}{\kappa_{\text{iso}}} = M \frac{\kappa}{\kappa_{\text{iso}}}. \quad (\text{C.7})$$

If $\bar{f} \approx \bar{f}_{\text{iso}}$ and $\tilde{f} \approx \frac{1}{3}$ are assumed, then $\frac{1}{2} \lesssim M \lesssim 2$ are reasonable bounds on M when considering the non-linear elastic properties reported for 10 cubic metals in (26).

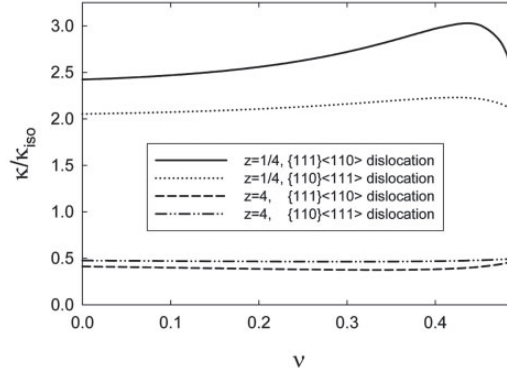


Fig. C.1 Energy factor for cubic crystal normalised by energy factor in isotropic solid

Considered now are mixed dislocations with tangent lines parallel to $[101]$. For a $\frac{1}{2}\langle 110\rangle\{111\}$ dislocation (typical in FCC crystals) and for a $\frac{1}{2}\langle 111\rangle\{110\}$ dislocation (typical in BCC), respectively (43),

$$\kappa = \frac{1}{4}(\kappa_1 + 2\kappa_2 + \kappa_3) \quad (\text{FCC}), \quad \kappa = \frac{1}{3}(\kappa_2 + 2\kappa_3) \quad (\text{BCC}); \quad (\text{C.8})$$

$$\kappa_1 = \left(\hat{C} + \frac{2\nu}{1-2\nu} \right) \left(\frac{z(1-2\nu)[\hat{C} - 2\nu/(1-2\nu)]}{(2-2\nu)[\hat{C} + 2\nu/(1-2\nu) + 2z]} \right) G, \quad (\text{C.9})$$

$$\kappa_2 = \kappa_1 \left[\frac{2-2\nu}{1+(1-2\nu)z} \right]^{1/2}, \quad \kappa_3 = z^{1/2}G, \quad \hat{C} = \left[\frac{2-2\nu}{1-2\nu} \left(\frac{1}{1-2\nu} + z \right) \right]^{1/2}. \quad (\text{C.10})$$

Ratio $\kappa/\kappa_{\text{iso}}$ depends only on dislocation type, ν , and z , noting that $z = 1$ for isotropic elasticity. Values of $\kappa/\kappa_{\text{iso}}$ are shown in Fig. C.1 over the range $0 \leq \nu \leq 0.49$ for anisotropy ratios $z = \frac{1}{4}$ and $z = 4$, properties which bound many cubic metals (for example, $z \approx 1.0$ for W (44), $z \approx 2.4$ for Fe (28), and $z \approx 3.2$ for Cu (45)), the alkali metals being a notable exception (45). From Fig. C.1, $\frac{1}{3} \lesssim \kappa/\kappa_{\text{iso}} \lesssim 3$. Combining this result with previously stated bounds on M yields, from (C.7), the estimate $\frac{1}{6} \lesssim \Delta V/\Delta V_{\text{iso}} \lesssim 6$. Relevance of the isotropic approximation used in Sections 3 and 4 to determine non-linear elastic contributions to \mathbf{F}^I can be assessed for a particular cubic crystal by substitution of its elastic properties into the above equations, or into analogous equations that can be derived using the same procedure with anisotropic energy factors available for other edge, screw, or mixed dislocation types (43).

NO. OF
COPIES ORGANIZATION

1 DEFENSE TECHNICAL
(PDF) INFORMATION CTR
DTIC OCA

2 DIRECTOR
(PDF) US ARMY RESEARCH LAB
RDRL CIO LL
IMAL HRA MAIL & RECORDS MGMT

1 GOV'T PRINTG OFC
(PDF) A MALHOTRA

34 DIR USARL
(PDF) RDRL CIH C
J KNAP
RDRL WM
R DONEY
B FORCH
J MCCAULEY
RDRL WML B
I BATYREV
B RICE
D TAYLOR
N WEINGARTEN
RDRL WML H
B SCHUSTER
RDRL WMM
J BEATTY
RDRL WMM B
G GAZONAS
C RANDOW
RDRL WMM E
J SWAB
RDRL WMM F
T SANO
M TSCHOPP
RDRL WMM G
J ANDZELM
RDRL WMP
S SCHOENFELD
RDRL WMP B
C HOPPEL
D POWELL
S SATAPATHY
M SCHEIDLER
T WEERISOORIYA
RDRL WMP C
R BECKER
S BILYK
T BJERKE
D CASEM
J CLAYTON
D DANDEKAR

NO. OF
COPIES ORGANIZATION

M GREENFIELD
R LEAVY
J LLOYD
M RAFTENBERG
S SEGLETES
C WILLIAMS

INTENTIONALLY LEFT BLANK.